

Mixed-Integer Programming for Change-point Detection

Apoorva Narula, Santanu S. Dey, Yao Xie

H. Milton Stewart School of Industrial and Systems Engineering (ISyE),
 Georgia Institute of Technology, USA
 {anarula34, santanu.dey, yao.xie}@gatech.edu

Abstract

We present a new mixed-integer programming (MIP) approach for offline multiple change-point detection by casting the problem as a globally optimal piecewise linear (PWL) fitting problem. Our main contribution is a family of strengthened MIP formulations whose linear programming (LP) relaxations admit integral projections onto the segment assignment variables, which encode the segment membership of each data point. This property yields provably tighter relaxations than existing formulations for offline multiple change-point detection. We further extend the framework to two settings of active research interest: (i) multidimensional PWL models with shared change-points, and (ii) sparse change-point detection, where only a subset of dimensions undergo structural change. Extensive computational experiments on benchmark real-world datasets demonstrate that the proposed formulations achieve reductions in solution times under both ℓ_1 and ℓ_2 loss functions in comparison to the state-of-the-art.

Keywords: piecewise linear function fitting; strengthened MIP formulations; integral LP projections; multidimensional fitting; sparse change-point detection.

1 Introduction

Piecewise linear (PWL) fitting involves partitioning ordered observations into contiguous segments, each modeled by a linear function, with the segment boundaries inferred from the data. PWL fitting can be interpreted as a form of change-point detection, where the goal is to identify locations at which either the intercept, the slope, or both parameters abruptly change. Such structural breaks arise in applications across healthcare (Tobiasz et al. [2023]), power systems (Buason et al. [2025], Ahmadi et al. [2013]), manufacturing (Gao et al. [2018]), public policy (Wagner et al. [2002], Dehning et al. [2020]), and other domains where detecting regime shifts is essential for interpretation and downstream decision-making. We consider an offline version of this task, in which the objective is to retrospectively identify locations where the structure of the underlying signal changes. A natural way to model this problem is through piecewise linear fitting, where each change-point corresponds to a boundary between linear segments. This representation provides a direct link between statistical change-point detection and optimization-based segmentation. Mixed-integer programming (MIP) provides an exact and globally optimal framework for offline PWL fitting. A key set of decision variables in such MIP formulations are the binary segment assignment variables, which indicate the segment each data point belongs to. Therefore, by explicitly encoding segment assignments, MIP formulations allow precise control over the number of structural changes. However, the practical scalability of MIP-based change-point detection is often limited by large runtimes, attributable in part to the weakness of the underlying linear programming (LP) relaxations, which admit fractional segment-assignment patterns and consequently lead to excessive branch-and-bound effort. To

address this limitation, this paper introduces strengthened MIP formulations tailored to offline PWL-based change-point detection. Our central contribution is a new formulation for partitioning data points into contiguous segments using an extended representation of the segment-assignment variables. We establish that the projection of the linear programming relaxation onto the space of these extended segment-assignment variables is integral. This eliminates broad classes of fractional solutions admitted by the LP relaxations of existing formulations, yielding a tighter relaxation without loss of modeling flexibility. Comprehensive computational experiments demonstrate that the proposed formulations consistently achieve global optimality faster than existing benchmarks. Moreover, the framework is shown to extend naturally to multidimensional and sparse offline change-point detection settings, illustrating the broader impact of formulation strengthening beyond the univariate case.

The main contributions of this work are summarized as follows:

- Strengthened mixed-integer programming formulations for offline change-point detection by piecewise linear fitting are developed, whose linear programming relaxations admit an integral projection onto the space of extended segment-assignment variables.
- A comprehensive computational study is conducted comparing the proposed formulations with existing MIP benchmarks, demonstrating consistent runtime improvements across multiple loss functions (the ℓ_1 and ℓ_2 error norms) and modeling regimes, including both continuous and non-continuous segment formulations and varying numbers of segments.
- The proposed framework is extended to two additional settings of active research interest: (i) multidimensional offline multiple change-point detection, and (ii) sparse change-point detection.

Throughout this paper, we use the term change-point to refer to a structural change in the underlying signal of the data, and the term breakpoint to denote the corresponding decision variable in a PWL model at which model parameters may change.

1.1 Literature Review

Advances in computational power and the improved scalability of commercial mixed-integer programming (MIP) solvers have enabled the application of MIP methodologies to increasingly large-scale statistical and machine-learning problems. Motivated by these developments, the present work studies the application of MIP to change-point detection using piecewise linear (PWL) fitting as a unifying framework across the various settings of this statistical problem. From an optimization perspective, the key combinatorial decision concerns the optimal partitioning of data points into contiguous segments. Consequently, the segment-assignment component of the overall PWL fitting MIP is of central importance, and it is essential to understand how existing formulations model this aspect. One of the earliest such formulations is given by Bertsimas and Shioda [2007], who assign observations to affine components using binary variables. In the univariate setting, this induces a form of piecewise linear fitting; however, contiguity of segment assignments is not enforced, and observations assigned to the same affine component need not be consecutive. As a result, although the model fits a fixed number of affine functions, it does not localize structural changes in the signal and does not distinguish between fitting multiple components and detecting change-points. Subsequent work expanded the scope of piecewise affine fitting to higher-dimensional domains. Toriello and Vielma [2012] develop MIP formulations based on interpolation over a fixed grid, yielding globally optimal solutions relative to a prescribed discretization but requiring the grid

to be specified in advance. To avoid explicit triangulation, Cui et al. [2018] represent the fitted function as the difference of two convex piecewise-affine components, resulting in a non-convex optimization problem. While these approaches address modeling challenges in higher dimensions, they do not directly target the segmentation structure required for change-point detection. More recent work focuses explicitly on the single-dimensional domain case and enforces contiguity of segments. Rebennack and Krasko [2020] and Goldberg et al. [2021] develop MIP-based formulations that encode segmentation decisions using binary variables and impose continuity of the fitted function, yielding globally optimal PWL fits well aligned with the requirements of change-point detection. A comparative study by Warwicker and Rebennack [2022] finds the formulation of Rebennack and Krasko [2020] to be the most computationally effective among existing MIP-based models, including Kong and Maravelias [2020]. Extensions include clustered regression settings Warwicker and Rebennack [2023] and formulations that minimize the number of segments subject to an approximation error tolerance Ploussard [2024]. A parallel line of research addresses change-point detection through penalization-based methods. In the single-response setting, Prokhorov et al. [2025] control the number of changes using an ℓ_0 penalty on parameter differences, while total-variation approaches such as Harchaoui and Lévy-Leduc [2010] detect mean changes using ℓ_1 penalization, and Zhang and Siegmund [2007] use a modified Bayesian information criterion (BIC) to select the number of mean shifts. These approaches are computationally attractive and statistically well studied, but they do not produce explicit segment assignments or breakpoint variables, which limits their ability to incorporate structural constraints and enforce shared change-points across multiple dimensions in the multivariate response setting. In multivariate settings, existing work primarily focuses on sparse mean shifts (Xie and Siegmund [2013], Cao et al. [2018], Wang and Samworth [2018]), typically without explicitly modeling piecewise linear structure or yielding globally optimal solutions under a unified segmentation framework. In the univariate sequence setting, our work, together with Rebennack and Krasko [2020] and Goldberg et al. [2021], models segmentation explicitly using binary decision variables while fixing the number of segments. This approach enforces contiguity of segment assignments, allows optional continuity of the fitted function, and restricts changes in slope and intercept to designated change-points represented by breakpoint variables. Building on this literature, this paper focuses on strengthening the segment-assignment component of MIP formulations for offline PWL-based change-point detection by introducing an extended formulation whose LP relaxation admits an integral projection onto the space of the extended segment-assignment variables. In addition to offline multiple change-point detection in the univariate response setting, we discuss extensions of this MIP framework to multiple change-point detection in multidimensional response settings and to sparse change-point detection scenarios. The remainder of the paper is organized as follows. Section 2 introduces the MIP formulations for one-dimensional piecewise-linear fitting. Section 3 establishes their theoretical properties based on the geometry of the polyhedra described by their associated LP relaxations. Section 4 extends the methodology to the multidimensional change-point detection and sparse change-point detection settings. Section 5 describes the computational experiments performed to empirically compare the runtime performance of the proposed formulations. Section 6 presents the results obtained from these experiments, and Section 7 offers concluding remarks and outlines directions for future research.

2 Multiple Change-Point Detection for Univariate Sequences

Given a dataset $\{(x_t, y_t)\}_{t=1}^T$ of T observations, where $y_t \in \mathbb{R}$ and $x_t \in \mathbb{R}^d$, we aim to fit a piecewise linear function $f : \mathbb{R}^d \rightarrow \mathbb{R}$ with K segments by minimizing a chosen error metric between the fitted

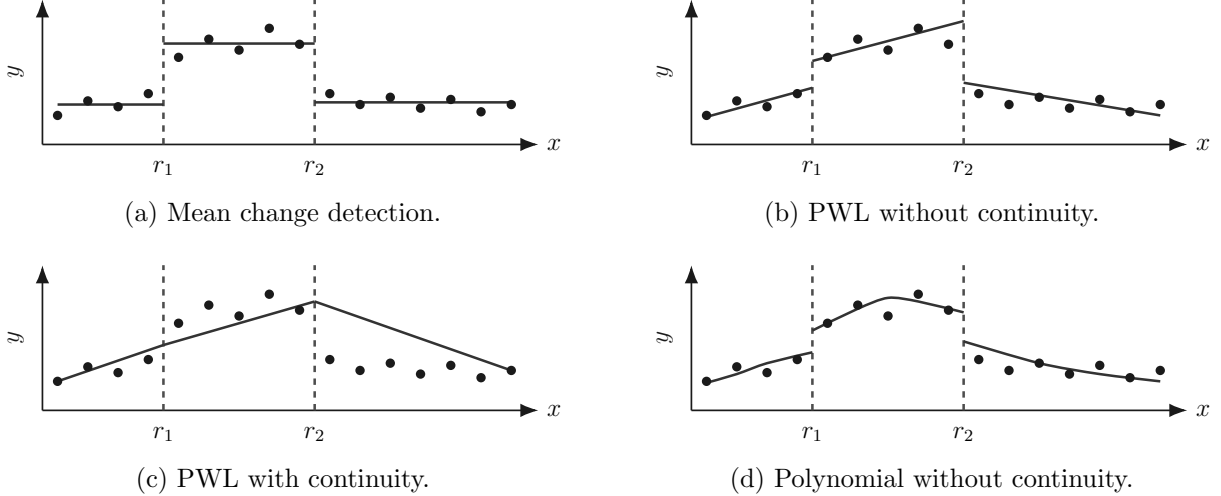


Figure 1: Illustrative change-point detection scenarios on the same underlying data: (a) mean change detection, (b) piecewise linear without continuity, (c) piecewise linear with continuity, (d) piecewise polynomial without continuity.

and observed responses. Here, x_t denotes the predictor variables. In simple time-series settings, x_t corresponds to the time index and thus takes positive integer values, as in uniformly sampled data; this is the setting considered throughout this work. However, the proposed methodology can be naturally extended to settings in which x_t does not lie on a positive integer grid, as in non-uniformly sampled time-series. Figure 1 illustrates several stylized piecewise fitting scenarios, including mean-shift segmentation, PWL fitting without continuity, PWL fitting with continuity, and piecewise polynomial fitting. Throughout this work, we focus on PWL models with and without continuity. We denote by \mathcal{F}_K the family of piecewise linear functions with K segments. Moreover, we restrict attention to the univariate domain case $d = 1$, so that $x_t \in \mathbb{R}$ for all t . Any function $f \in \mathcal{F}_K$ admits the parametric representation as described below.

$$f(x \mid \boldsymbol{\theta}) = \begin{cases} m_1 x + c_1, & x \in [r_0, r_1], \\ m_2 x + c_2, & x \in (r_1, r_2], \\ \vdots \\ m_{K-1} x + c_{K-1}, & x \in (r_{K-2}, r_{K-1}], \\ m_K x + c_K, & x \in (r_{K-1}, r_K], \end{cases}$$

where the parameter vector

$$\boldsymbol{\theta} = (\{m_i, c_i\}_{i=1}^K, r_0, r_1, \dots, r_K)$$

contains the segment slopes, intercepts, and breakpoint locations. The breakpoints satisfy $r_0 \leq r_1 \leq \dots \leq r_K$ and correspond to locations in the domain at which the fitted function may change either its slope, its intercept, or both. We assume that $\boldsymbol{\theta}$ belongs to a parameter space Θ , which imposes lower and upper bounds on the slopes, intercepts, and breakpoint locations based on the observed data. The parameter space Θ considered in this work is similar to that used by Rebennack and Krasko [2020], further details on the construction of Θ are provided in Appendix A.1. Given the function class \mathcal{F}_K , the fitting problem is formulated as

$$\min_{f \in \mathcal{F}_K} \sum_{t=1}^T |y_t - f(x_t)|^q, \quad q \in \{1, 2\},$$

where $q = 1$ corresponds to minimizing the ℓ_1 loss and $q = 2$ corresponds to minimizing the squared ℓ_2 loss. Optionally, we may require the fitted function to be continuous across segment boundaries. Continuity is enforced by the constraints

$$m_i r_i + c_i = m_{i+1} r_i + c_{i+1}, \quad i = 1, \dots, K-1.$$

By convention, we set $r_0 = x_1$ and $r_K = x_T$. Thus, the representation of a K segment PWL fitting requires $K+1$ breakpoints, of which two (namely, r_0 and r_K) are fixed. In the MIP-based change-point detection literature (e.g., Goldberg et al. [2021], Rebennack and Krasko [2020]), continuity of the fitted function at each change-point is typically enforced. However, the statistical change-point literature does not generally impose continuity since a change may manifest as a jump discontinuity, a change in slope, or both. In many practical settings it is not reasonable to assume a priori that the underlying signal remains continuous after a structural change, while in other applications continuity may indeed be warranted due to physical or engineering constraints. Motivated by these considerations, both continuous and discontinuous PWL models are studied in the univariate sequence setting. This choice enables a fair comparison between the proposed MIP formulations and existing benchmark methods, which consider this setting. In contrast, for multidimensional and sparse change-point detection settings, continuity is not imposed, as is consistent with the literature in these fields. In the remainder of this work, we refer to the MIP formulations proposed by Goldberg et al. [2021] and Rebennack and Krasko [2020] as the Basic and Alternate formulations, respectively. We introduce modular extensions to the segment-assignment components of each of these models, and accordingly refer to our proposed methods as the Extended Basic and Extended Alternate formulations.

2.1 Basic MIP Formulation

The formulation of Goldberg et al. [2021] relies on binary segment-assignment variables to encode the partition of the data into linear segments. The complete Basic formulation minimizes the total fitting error under the chosen ℓ_q norm, subject to the decision variables and constraints listed below.

Decision variables and parameters

- Segment-assignment variables: For each segment $j \in \{1, \dots, K\}$ and observation $t \in \{1, \dots, T\}$, let

$$\delta_{j,t} \in \{0, 1\}$$

be a binary variable indicating segment membership, where $\delta_{j,t} = 1$ if observation t is assigned to segment j . These variables encode the partitioning of the data into K contiguous segments.

- Segment parameters: For each segment $j \in \{1, \dots, K\}$, let

$$m_j \in \mathbb{R}, \quad c_j \in \mathbb{R}$$

denote the slope and intercept respectively, of the linear function associated with segment j .

- Breakpoint variables: Let

$$r_j \in \mathbb{R}, \quad j = 0, 1, \dots, K,$$

denote the breakpoint locations defining the segment boundaries. The breakpoint locations follow the same order as the corresponding segments; therefore, $r_j \leq r_{j+1}$ for all j . By convention, $r_0 = x_1$ and $r_K = x_T$.

- Fitted values: For each observation $t \in \{1, \dots, T\}$, let

$$\hat{y}_t \in \mathbb{R}$$

denote the fitted response value produced by the model at input x_t .

- Big- M parameters: The formulation uses nonnegative constants

$$M_{1,t}^A, \quad M_{2,t}^A, \quad M_{3,t}^A, \quad t = 1, \dots, T,$$

which serve as big- M parameters used to deactivate constraints when $\delta_{j,t} = 0$. Specifically:

- $M_{1,t}^A$ relaxes the value-assignment constraints (2.1.2) - (2.1.3), allowing the linear function of segment j to differ from \hat{y}_t when observation t is not assigned to segment j .
- $M_{2,t}^A$ and $M_{3,t}^A$ relax the breakpoint localization constraints (2.1.4) - (2.1.5), ensuring that the bounds imposed by breakpoints r_j and r_{j+1} are enforced only for the active segment.

The derivation of these constants is discussed in Appendix A.1.

Objective function

$$\min \sum_{t=1}^T |y_t - \hat{y}_t|^q, \quad q \in \{1, 2\},$$

Constraints

(A1) Basic segment-assignment constraints: Each observation must be assigned to exactly one segment.

$$\sum_{j=1}^K \delta_{j,t} = 1, \quad \forall t = 1, \dots, T. \quad (2.1.1)$$

(A2) Value assignment constraints: The fitted value \hat{y}_t must coincide with the linear function associated with segment j whenever $\delta_{j,t} = 1$. Hence, for each segment $j \in \{1, \dots, K\}$ and observation $t \in \{1, \dots, T\}$:

$$m_j x_t + c_j \leq \hat{y}_t + M_{1,t}^A (1 - \delta_{j,t}), \quad (2.1.2)$$

$$m_j x_t + c_j \geq \hat{y}_t - M_{1,t}^A (1 - \delta_{j,t}). \quad (2.1.3)$$

(A3) Breakpoint localization constraints: The breakpoints r_{j-1} and r_j must bound all observations assigned to segment j . Hence, for each segment $j \in \{1, \dots, K\}$ and observation $t \in \{1, \dots, T\}$:

$$x_t \leq r_j + M_{2,t}^A (1 - \delta_{j,t}), \quad (2.1.4)$$

$$x_t \geq r_{j-1} - M_{3,t}^A (1 - \delta_{j,t}), \quad (2.1.5)$$

with fixed endpoint conditions

$$r_0 = x_1, \quad r_K = x_T. \quad (2.1.6)$$

and the breakpoints are required to be non-decreasing in the segment index:

$$r_j \leq r_{j+1}, \quad \forall j = 0, \dots, K-1. \quad (2.1.7)$$

The presence of these breakpoints, which provide upper and lower bounds on all x_t assigned to a segment, together with their nondecreasing order, leads to the assignment of points to segments in a contiguous manner.

(A4) Basic continuity constraints (optional): To enforce continuity of the fitted function across adjacent segments, the following constraint is imposed.

$$m_j r_j + c_j = m_{j+1} r_j + c_{j+1}, \quad \forall j = 1, \dots, K-1. \quad (2.1.8)$$

(A5) Variable domains and parameter bounds: The decision variables and parameters are restricted to the parameter space Θ , which imposes bounds based on the observed data.

$$\begin{aligned} m_j &\in [L^m, U^m] \subset \mathbb{R}, & \forall j \in \{1, \dots, K\}, \\ c_j &\in [L^c, U^c] \subset \mathbb{R}, & \forall j \in \{1, \dots, K\}, \\ \hat{y}_t &\in \mathbb{R}, & \forall t \in \{1, \dots, T\}, \\ \delta_{j,t} &\in \{0, 1\}, & \forall j \in \{1, \dots, K\}, \forall t \in \{1, \dots, T\}. \end{aligned} \quad (2.1.9)$$

The construction of Θ and the associated big- M constants $M_{1,t}^A$, $M_{2,t}^A$, and $M_{3,t}^A$ is discussed in detail in Appendix A.1, which uses the same derivation as Rebennack and Krasko [2020].

2.2 Alternate MIP Formulation

We next describe the Alternate formulation of Rebennack and Krasko [2020]. This formulation replaces the bilinear continuity constraints of the Basic model with linear constraints that enforce continuity indirectly, without introducing explicit breakpoint decision variables. Continuity is instead modeled by introducing additional variables that capture changes in slope between successive linear segments, as discussed further in Remark 2. Consequently, two constraint blocks differ from the Basic formulation, namely the segment-assignment constraints and the continuity constraints. We therefore refer to them as the Alternate segment-assignment constraints and the Alternate continuity constraints.

Additional decision variables and parameters: In addition to the decision variables introduced in the Basic formulation, the Alternate formulation uses the following variables and parameters.

- Slope-direction indicators: For each segment $j \in \{1, \dots, K-1\}$, let

$$\gamma_j \in \{0, 1\}$$

be a binary variable indicating the direction of slope change between segments j and $j+1$. Specifically, $\gamma_j = 1$ corresponds to a non-increasing change in slope, i.e., $m_{j+1} \leq m_j$, while $\gamma_j = 0$ corresponds to a non-decreasing change in slope, i.e., $m_{j+1} \geq m_j$.

- Continuity-activation variables: For each segment $j \in \{1, \dots, K-1\}$ and observation $t \in \{1, \dots, T-1\}$, let

$$\delta_{j,t}^+, \delta_{j,t}^- \in [0, 1]$$

be continuous activation variables that control which linearized continuity constraints are enforced, depending on the direction of change in slope, indicated by γ_j .

- Big- M parameters: The Alternate formulation uses nonnegative constants

$$M_{4,t}^B, \quad t = 1, \dots, T,$$

which serve as big- M parameters in the linearized continuity constraints (2.2.5) - (2.2.10). These constants relax the continuity inequalities when the corresponding activation variables are inactive, ensuring validity of the formulation. Their derivation is elaborated in Appendix A.1, and is same as that proposed in Rebennack and Krasko [2020].

Constraints.

(B1) Alternate segment-assignment constraints:

$$\sum_{j=1}^K \delta_{j,t} = 1, \quad \forall t = 1, \dots, T, \quad (2.2.1)$$

$$\delta_{j+1,t+1} \leq \delta_{j,t} + \delta_{j+1,t}, \quad \forall j = 1, \dots, K-1, \forall t = 1, \dots, T-1, \quad (2.2.2)$$

$$\delta_{1,t+1} \leq \delta_{1,t}, \quad \forall t = 1, \dots, T-1, \quad (2.2.3)$$

$$\delta_{K,t+1} \geq \delta_{K,t}, \quad \forall t = 1, \dots, T-1. \quad (2.2.4)$$

(B2) Alternate continuity constraints: For all $j = 1, \dots, K-1$ and $t = 1, \dots, T-1$, the following inequalities enforce continuity of the fitted function in a linearized manner:

$$c_{j+1} - c_j \geq x_t(m_j - m_{j+1}) - M_{4,t}^B(1 - \delta_{j,t}^+), \quad (2.2.5)$$

$$c_{j+1} - c_j \leq x_{t+1}(m_j - m_{j+1}) + M_{4,t+1}^B(1 - \delta_{j,t}^+), \quad (2.2.6)$$

$$c_{j+1} - c_j \leq x_t(m_j - m_{j+1}) + M_{4,t}^B(1 - \delta_{j,t}^-), \quad (2.2.7)$$

$$c_{j+1} - c_j \geq x_{t+1}(m_j - m_{j+1}) - M_{4,t+1}^B(1 - \delta_{j,t}^-), \quad (2.2.8)$$

where the activation variables are governed by

$$\delta_{j,t} + \delta_{j+1,t+1} + \gamma_j - 2 \leq \delta_{j,t}^+, \quad (2.2.9)$$

$$\delta_{j,t} + \delta_{j+1,t+1} + (1 - \gamma_j) - 2 \leq \delta_{j,t}^-. \quad (2.2.10)$$

Remark 1 (Alternate Method of Contiguous Segment Assignment). Unlike the Basic formulation, in which contiguity of segment assignments is enforced through explicit breakpoint variables, contiguity here is achieved directly using the segment-assignment variables. For the case of two segments ($K = 2$), contiguity follows immediately from constraints (2.2.1), (2.2.3), and (2.2.4). This construction naturally extends to larger values of K , as discussed below. We show that any non-contiguous assignment for segment $j > 1$ necessarily induces a non-contiguous assignment for segment $j-1$. Suppose that $\delta_{j,t} = 1$ for

$$t \in \{T_1, \dots, T_1 + p_1\} \quad \text{and} \quad t \in \{T_1 + p_1 + p_2, \dots, T_1 + p_1 + p_2 + p_3\},$$

where p_1, p_2, p_3 are positive integers with $p_2 > 0$. Since $\delta_{1,1} = 1$ and exactly one segment can be assigned to each observation by (2.2.1), it follows that $T_1 > 1$. For such an assignment to be feasible, constraint (2.2.2) must be satisfied. This requires

$$\delta_{j-1,T_1-1} = 1 \quad \text{and} \quad \delta_{j-1,T_1+p_1+p_2-1} = 1,$$

while $\delta_{j-1,t} = 0$ whenever $\delta_{j,t} = 1$. In particular, $\delta_{j-1,t} = 0$ for all $t \in \{T_1, \dots, T_1 + p_1\}$, implying that segment $j-1$ is also assigned non-contiguously. Since the case $K = 2$ admits only contiguous segment assignments, this argument extends inductively to all positive integer values of K , establishing that the proposed constraints enforce contiguity of segment assignments.

Remark 2 (Alternate Method of Modeling Continuity). Suppose a breakpoint r occurs between observations x_t , assigned to segment j , and x_{t+1} , assigned to segment $j+1$. Continuity at the breakpoint requires that the two linear segments intersect at r , i.e.,

$$m_j r + c_j = m_{j+1} r + c_{j+1}.$$

Solving for r yields

$$r = \frac{c_{j+1} - c_j}{m_j - m_{j+1}}.$$

Since the breakpoint lies between x_t and x_{t+1} , it must satisfy

$$x_t \leq \frac{c_{j+1} - c_j}{m_j - m_{j+1}} \leq x_{t+1}.$$

If $m_j - m_{j+1} \geq 0$, this condition can be equivalently written as

$$x_t(m_j - m_{j+1}) \leq c_{j+1} - c_j \leq x_{t+1}(m_j - m_{j+1}),$$

which is modeled by constraints (2.2.5)–(2.2.6). If instead $m_j - m_{j+1} < 0$, the inequalities reverse, yielding

$$x_t(m_j - m_{j+1}) \geq c_{j+1} - c_j \geq x_{t+1}(m_j - m_{j+1}),$$

as represented by constraints (2.2.7) - (2.2.8). The activation of these constraints is governed by the segment-assignment variables. When a breakpoint occurs between observations t and $t + 1$, the assignments satisfy $\delta_{j,t} = 1$ and $\delta_{j+1,t+1} = 1$. The direction of the slope change between segments j and $j + 1$, encoded by γ_j , determines which pair of linearized continuity constraints is enforced. If $m_{j+1} \leq m_j$, then $\gamma_j = 1$, and constraint (2.2.9) forces $\delta_{j,t}^+ = 1$. In this case, the big- M terms in constraints (2.2.5)–(2.2.6) vanish, enforcing continuity at the breakpoint. Conversely, if $m_{j+1} \geq m_j$, then $\gamma_j = 0$, and constraint (2.2.10) forces $\delta_{j,t}^- = 1$, activating constraints (2.2.7)–(2.2.8) instead. Thus, exactly one pair of continuity constraints is activated at each breakpoint, depending on the relative ordering of the slopes of the adjacent segments.

2.3 Proposed Extended Formulations

We now introduce the proposed formulation for enforcing contiguous segment assignment that replaces the segment-assignment constraint blocks of both the Basic and Alternate formulations. The key idea is to construct segment membership from a family of nested, monotonically nonincreasing binary vectors

$$X_{j,\cdot} = (X_{j,1}, \dots, X_{j,T}), \quad j = 1, \dots, K - 1.$$

For each $j \in \{1, \dots, K - 1\}$ and $t \in \{1, \dots, T\}$, the binary variable

$$X_{j,t} \in \{0, 1\}$$

indicates whether observation t lies to the left of the activation boundary of segment $j + 1$. Specifically, $X_{j,t} = 1$ signifies that observation t is assigned to one of the first j segments, while $X_{j,t} = 0$ indicates that observation t belongs to segment $j + 1$ or later. The transition point at which $X_{j,t}$ switches from 1 to 0 therefore identifies the starting index of segment $j + 1$. The collection of vectors $\{X_{j,\cdot}\}_{j=1}^{K-1}$ is required to be nested and monotonically nonincreasing, ensuring that each segment boundary is activated at most once and that segment boundaries occur in increasing order. The segment-assignment variables $\delta_{j,t}$ are then derived from differences of the nested vectors, yielding contiguous and ordered segment blocks. The relationship between $X_{j,t}$ and the resulting $\delta_{j,t}$ is illustrated in Figure 2.

(C1) Extended segment-assignment constraints: The segment-assignment variables $\delta_{j,t}$ are defined in terms of the nested binaries $X_{j,t}$ as stated below.

$$\delta_{j,t} = \begin{cases} X_{1,t}, & j = 1, \\ X_{j,t} - X_{j-1,t}, & j = 2, \dots, K-1, \\ 1 - X_{K-1,t}, & j = K, \end{cases} \quad \forall j = 1, \dots, K, \forall t = 1, \dots, T. \quad (2.3.1)$$

To ensure consistent ordering across both segment and time indices, the nested vectors satisfy

$$X_{j,t} \geq X_{j,t+1}, \quad \forall j = 1, \dots, K-1, \forall t = 1, \dots, T-1, \quad (2.3.2)$$

$$X_{j+1,t} \geq X_{j,t}, \quad \forall j = 1, \dots, K-2, \forall t = 1, \dots, T. \quad (2.3.3)$$

Together, (2.3.1)–(2.3.3) guarantee that each segment is associated with a single contiguous block of data points and that segments activate in increasing order from 1 to K .

Replacing the basic segment-assignment block (A1) (constraint (2.1.1)) with the extended block (C1) (constraints (2.3.1)–(2.3.3)) yields the Extended Basic formulation. Similarly, replacing the Alternate segment-assignment block (B1) (constraints (2.2.1)–(2.2.4)) with block (C1) yields the Extended Alternate formulation. All remaining constraints of the respective formulations remain unchanged.

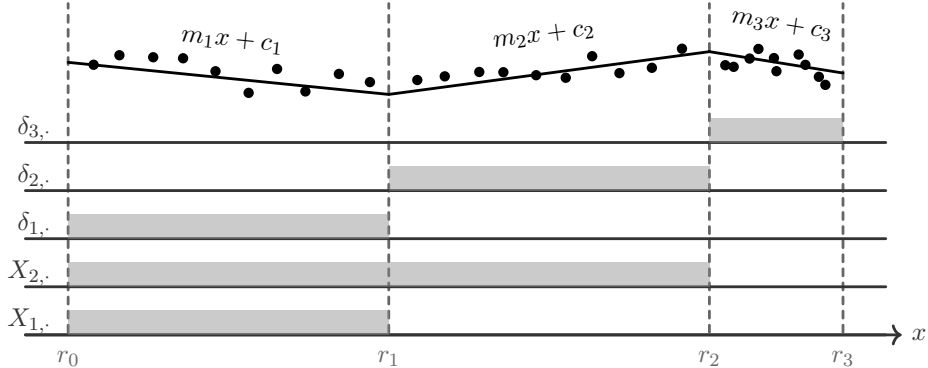


Figure 2: Illustration of how nested binary vectors $X_{1,..}$ and $X_{2,..}$ determine the segment-assignment variables $\delta_{1,..}, \delta_{2,..}, \delta_{3,..}$ in a continuous three-segment piecewise-linear fit. The vectors $X_{1,..}$ and $X_{2,..}$ are temporally nonincreasing. This yields $\delta_{1,..} = X_{1,..}$, $\delta_{2,..} = X_{2,..} - X_{1,..}$, and $\delta_{3,..} = 1 - X_{2,..}$, producing three contiguous segment blocks and the three piecewise linear segments $m_1x + c_1$, $m_2x + c_2$, and $m_3x + c_3$.

Remark 3 (Equivalence of the Basic and Extended Basic Formulations). The Basic and Extended Basic formulations define identical feasible regions. As stated earlier, the two models differ only in their treatment of segment-assignment constraints: the Basic formulation enforces segment contiguity through the block (A1) (constraint (2.1.1)), whereas the Extended Basic formulation replaces this block with the extended segment-assignment constraints (C1) (constraints (2.3.1)–(2.3.3)). We first show that every feasible solution to the Extended Basic formulation is feasible for the Basic formulation. Summing constraint (2.3.1) over the segment index j recovers constraint (2.1.1). Since all remaining constraints are identical in the two formulations, any solution feasible for the Extended Basic formulation satisfies all constraints of the Basic formulation. Conversely, we show

that every feasible solution to the Basic formulation is feasible for the Extended Basic formulation. Suppose, for the sake of contradiction, that there exists a solution that is feasible for the Basic formulation but infeasible for the Extended Basic formulation. Since all other constraints are common to both formulations, any infeasibility must arise from the extended segment-assignment constraints. However, the Basic formulation enforces that segment assignments induce contiguous partitions of the data indices. By construction, every contiguous partition admits a representation using the extended segment-assignment variables, which are derived from a set of monotonically nonincreasing, nested binary variable X vectors. Therefore, any segment assignment feasible in the Basic formulation can be encoded in a way that satisfies constraints (2.3.1)-(2.3.3), contradicting the assumed infeasibility. Hence, the feasible regions of the Basic and Extended Basic formulations coincide, and the two formulations are equivalent.

Remark 4 (Feasible-Region of the Alternate formulation is strictly contained in that of the Extended Alternate Formulation). The Alternate and Extended Alternate formulations differ only in their segment-assignment constraints. The Alternate formulation enforces contiguity through the block (B1) (constraints (2.2.1) - (2.2.4)), whereas replacing this block with the extended segment-assignment constraints (C1) yields the Extended Alternate formulation. Every feasible solution to the Alternate formulation is also feasible for the Extended Alternate formulation since the Alternate formulation admits only contiguous partitions of the data indices, and every such contiguous partition can be represented using the extended segment-assignment variables satisfying constraints (C1). Thus, the feasible region of the Alternate formulation is contained within that of the Extended Alternate formulation. However, the reverse inclusion does not hold. There exist segment assignments that are feasible under the extended segment-assignment constraints but infeasible under the Alternate formulation. To illustrate this, consider the following assignment of the segment variables:

$$\begin{aligned}\delta_{1,.} &= [1, 1, 0, 0, 0, 0, 0, 0, 0], \\ \delta_{2,.} &= [0, 0, 1, 1, 1, 0, 0, 0, 0], \\ \delta_{3,.} &= [0, 0, 0, 0, 0, 0, 0, 0, 0], \\ \delta_{4,.} &= [0, 0, 0, 0, 0, 1, 1, 0, 0], \\ \delta_{5,.} &= [0, 0, 0, 0, 0, 0, 0, 1, 1].\end{aligned}$$

This assignment satisfies the extended segment-assignment constraints (2.3.1) - (2.3.3). However, it violates the Alternate contiguity constraint (2.2.2). Specifically, setting $(j, t) = (3, 5)$ in (2.2.2) yields

$$\delta_{4,6} \leq \delta_{3,5} + \delta_{4,5} = 0,$$

whereas $\delta_{4,6} = 1$, resulting in a violation. The violation arises because segment 3 is unused, i.e., no data points are assigned to it, despite the model allowing up to five segments. Such assignments are permitted by the Extended Alternate formulation, which allows unused segments, but are excluded by the Alternate formulation, whose contiguity constraints implicitly enforce the use of all segments. Consequently, the feasible region of the Extended Alternate formulation strictly contains that of the Alternate formulation.

Remark 5 (Allowing Unused Segments and ℓ_0 -Regularized PWL Fitting). Based on Remark 4, the Extended Alternate formulation admits feasible piecewise linear fits in which some of the available segments remain unused. By Remark 3, the Basic and Extended Basic formulations are equivalent, and therefore the Basic formulation also permits such solutions. As a consequence, the Basic, Extended Basic, and Extended Alternate formulations can be employed to perform piecewise linear fitting while allowing the number of active segments to be selected by the model through ℓ_0 -type

regularization that penalizes the number of segments actually used in the fit, thereby preventing overfitting. In this setting, the parameter K serves as an upper bound on the number of segments, instead of the exact number of segments to be fitted. This flexibility facilitates model selection within this mixed-integer programming framework. An explicit MIP formulation for ℓ_0 -regularized piecewise linear fitting is presented in Appendix A.2.

Remark 6 (Same Optimal Solution for the Basic, Alternate, and Extended Formulations). All of these formulations partition the data indices into a fixed number of contiguous segments and perform piecewise linear fitting, with or without continuity constraints, by minimizing either the ℓ_1 or the ℓ_2 error norm. Although the formulations differ in their segment-assignment and continuity constraints, every admissible piecewise linear fit corresponds to a feasible solution in each formulation. Conversely, every feasible solution to any of these formulations induces a valid piecewise linear fit with the prescribed number of segments. Since the global optimum is determined by the piecewise linear fit that minimizes the chosen error norm, this optimal fit admits a feasible and optimal representation in all formulations. While the internal variable representations may differ, all formulations achieve the same optimal objective value and the same fitted function.

3 Comparison using Polyhedral Theory

We study the polyhedral structure of the change-point detection MIP formulations introduced in Section 2. Our objective is to provide theoretical insight into their relative computational performance by analyzing the geometry of their feasible regions. Although the formulations differ in their constraint sets and variable spaces, they all model the same underlying combinatorial problem of partitioning the data points into contiguous segments. Consequently, all formulations share the common set of segment-assignment variables. Accordingly, we compare the formulations using two polyhedral viewpoints. First, we compare the Basic and Extended Basic formulations by examining the projection of their LP relaxations onto the shared δ -variable space. Second, we analyze the polyhedral structure induced by individual segment-assignment blocks. In particular, we study the integrality of the polyhedron defined by the extended block (C1) together with relaxed binary bounds, and we show that the polyhedron defined by the alternate block (B1) with relaxed binary bounds is not integral. Throughout this section, we distinguish between binary decision variables and their LP-relaxed counterparts using a superscript “ \sim ”. Specifically, the LP relaxations of the variables X and δ are denoted by \tilde{X} and $\tilde{\delta}$, respectively. We consider a K -segment fitting problem with index sets

$$i \in \{1, \dots, K-1\}, \quad j \in \{1, \dots, K\}, \quad t \in \{1, \dots, T\}.$$

The original binary variables and their LP relaxations satisfy

$$\begin{aligned} X_{i,t} &\in \{0, 1\}, & \tilde{X}_{i,t} &\in [0, 1], \\ \delta_{j,t} &\in \{0, 1\}, & \tilde{\delta}_{j,t} &\in [0, 1]. \end{aligned}$$

All constraints in the segment-assignment block (2.3.1)–(2.3.3) are imposed identically on both the integer variables and their LP-relaxed counterparts. We begin by providing some theoretical framework which will be used later in the section.

Definition 3.1 (Integral Polytope). A polytope $P \subseteq \mathbb{R}^n$ is called integral if all of its vertices are integer-valued.

Definition 3.2 (Projection of a Polyhedron). Let $P \subseteq \mathbb{R}^{n+m}$ be a polyhedron defined over variables (x, y) , i.e.,

$$P = \{(x, y) \in \mathbb{R}^{n+m} : Ax + By \leq b\}.$$

The projection of P onto the y -space is the polyhedron

$$\text{proj}_y(P) = \{y \in \mathbb{R}^m : \exists x \in \mathbb{R}^n \text{ such that } (x, y) \in P\}.$$

Definition 3.3 (Total Variation). Let $f : [a, b] \rightarrow \mathbb{R}$ be a real-valued function. The total variation of f on $[a, b]$ is defined as

$$\text{TV}(f) := \sup_{\mathcal{P}} \sum_{i=1}^n |f(x_i) - f(x_{i-1})|,$$

where the supremum is taken over all finite partitions

$$\mathcal{P} = \{a = x_0 < x_1 < \dots < x_n = b\}$$

of the interval $[a, b]$. A function f is said to have bounded variation on $[a, b]$ if $\text{TV}(f) < \infty$.

Lemma 3.4 (Total Variation Bound for Differences). *Let $f, g : [a, b] \rightarrow \mathbb{R}$ be functions of bounded variation, and define $h = f - g$. Then h also has bounded variation and satisfies*

$$\text{TV}(h) \leq \text{TV}(f) + \text{TV}(g).$$

Proof. For any finite partition $\mathcal{P} = \{x_0 < x_1 < \dots < x_n\}$ of $[a, b]$, we have

$$\begin{aligned} \sum_{i=1}^n |h(x_i) - h(x_{i-1})| &= \sum_{i=1}^n |(f(x_i) - f(x_{i-1})) - (g(x_i) - g(x_{i-1}))| \\ &\leq \sum_{i=1}^n |f(x_i) - f(x_{i-1})| + \sum_{i=1}^n |g(x_i) - g(x_{i-1})|. \end{aligned}$$

Taking the supremum over all finite partitions \mathcal{P} yields the result. \square

Remark 7 (Total Variation on a Finite or Countable Support). When f is defined on a finite or countable ordered support $\{t_1 < t_2 < \dots < t_T\} \subset \mathbb{R}$, its total variation is naturally defined as

$$\text{TV}(f) := \sum_{t=2}^T |f(t) - f(t-1)|.$$

This discrete definition coincides with the continuous definition in Definition 3.3 when f is extended to a right-continuous piecewise constant function on $[t_1, t_T]$.

Proposition 1 (Strict Containment of the Extended Basic Projection). *Let Q and P denote the polytopes obtained by projecting the LP relaxations of the Basic and Extended Basic formulations, respectively, onto the δ -variable space (i.e., the set of all fractional segment-assignment vectors $\hat{\delta}$ that satisfy the LP relaxations of the corresponding formulations). Then*

$$P \subsetneq Q.$$

Proof. The Basic and Extended Basic formulations differ only in their segment-assignment blocks. Specifically, constraint set (A1) (2.1.1) in the Basic formulation is replaced by constraint set (C1) ((2.3.1)–(2.3.3)) in the Extended Basic formulation. By construction, every feasible solution to the LP relaxation of (C1) induces a relaxed segment-assignment vector $\tilde{\delta}$ that satisfies the Basic constraint

$$\sum_{j=1}^K \tilde{\delta}_{j,t} = 1 \quad \forall t.$$

This is because summing constraint (2.3.1) over the segment index j yields (2.1.1). Hence, every $\tilde{\delta}$ feasible under the Extended Basic relaxation is also feasible under the Basic relaxation, implying $P \subseteq Q$. To show that this inclusion is strict, we demonstrate that there exist $\tilde{\delta}$ -patterns that satisfy the Basic LP relaxation but cannot arise from any feasible solution of constraint set (C1). The key observation is that the relaxed variables $\tilde{X}_{j,t}$ appearing in (C1) form nested, monotonically nonincreasing relaxed binary sequences as a consequence of constraints (2.3.2)–(2.3.3). This imposes a restriction on the total variation of differences between such sequences. We apply Lemma 3.4 to the sequences $\{\tilde{X}_{j,t}\}_{t=1}^T$. Since each $\tilde{X}_{j,\cdot}$ is binary and nonincreasing in t , its total variation satisfies

$$\text{TV}(\tilde{X}_{j,\cdot}) = 1.$$

For $j = 2, \dots, K-1$, the relaxed segment-assignment variables satisfy

$$\tilde{\delta}_{j,t} = \tilde{X}_{j,t} - \tilde{X}_{j-1,t}.$$

Therefore, by Lemma 3.4,

$$\text{TV}(\tilde{\delta}_{j,\cdot}) \leq \text{TV}(\tilde{X}_{j,\cdot}) + \text{TV}(\tilde{X}_{j-1,\cdot}) = 2.$$

Consequently, any $\tilde{\delta}$ -sequence whose total variation exceeds 2 cannot be expressed as the difference of two nested monotonically nonincreasing binary sequences and is thus infeasible under constraint set (C1), even though it may satisfy the Basic relaxation. Figure 3 provides an explicit example in which the sequences $\tilde{\delta}_{2,\cdot}$ and $\tilde{\delta}_{3,\cdot}$ attain total variation exceeding 2, rendering them infeasible for the Extended Basic relaxation while remaining feasible for the Basic relaxation. The corresponding segment-assignment vectors are:

$$\begin{aligned} \tilde{\delta}_{1,\cdot} &= [0.5, 0.5, 0.5, 0.5, 0.5, 0.5, 0.5, 0.5], \\ \tilde{\delta}_{2,\cdot} &= [0.4, 0.1, 0.4, 0.1, 0.4, 0.1, 0.4, 0.1], \\ \tilde{\delta}_{3,\cdot} &= [0.1, 0.4, 0.1, 0.4, 0.1, 0.4, 0.1, 0.4], \\ \tilde{\delta}_{4,\cdot} &= [0, 0, 0, 0, 0, 0, 0, 0]. \end{aligned}$$

As shown in Appendix A.3, this $\tilde{\delta}$ provides a complete feasible solution satisfying all the constraints of the Basic formulation. Hence, $P \subsetneq Q$, and the inclusion is strict. \square

Proposition 2 (Integrality of the (C1) Polyhedron). *Let R denote the polyhedron defined by the constraint set (C1), i.e., constraints (2.3.1)–(2.3.3), together with the integrality relaxed variable bounds for these binary variables*

$$\tilde{X}_{j,t} \in [0, 1], \quad \tilde{\delta}_{j,t} \in [0, 1], \quad \forall j = 1, \dots, K, t = 1, \dots, T.$$

Then the polyhedron R is integral.

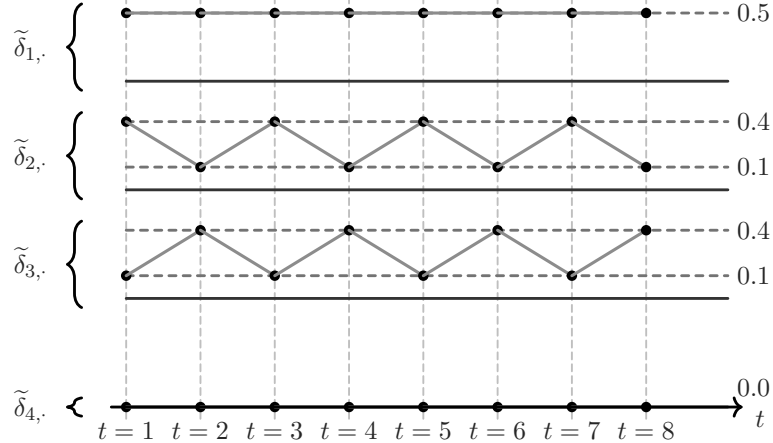


Figure 3: Configuration that is feasible for the LP relaxations of the Basic and Alternate formulations but infeasible for their extended counterparts, as the sequences $\tilde{\delta}_{2,\cdot}$ and $\tilde{\delta}_{3,\cdot}$ violate the total-variation bound implied by $\tilde{\delta}_{j,t} = \tilde{X}_{j,t} - \tilde{X}_{j-1,t}$.

Proof. Consider the constraint matrix associated with the constraints in (C1), expressed in the variables $\{\tilde{X}_{j,t}, \tilde{\delta}_{j,t}\}$. After a suitable permutation of columns, this matrix can be written in block form as follows.

1. The constraints (2.3.1) induce coefficients on the $\tilde{\delta}_{j,t}$ variables that form an identity submatrix.
2. The constraints (2.3.1) - (2.3.3) induce coefficients on the $\tilde{X}_{j,t}$ variables such that each row contains at most two nonzero entries, each equal to $+1$ or -1 , and whenever two nonzero entries appear in a row, they have opposite signs. Constraint matrices with this structure are well known to be totally unimodular.

Total unimodularity is preserved under column permutations and under horizontal concatenation with an identity matrix. Consequently, the full constraint matrix associated with (C1) is totally unimodular. In addition, the variable bound constraints

$$0 \leq \tilde{X}_{j,t} \leq 1, \quad 0 \leq \tilde{\delta}_{j,t} \leq 1,$$

can be written explicitly as linear inequalities whose coefficient matrices are identity matrices (up to sign). In particular,

$$\tilde{X}_{j,t} \leq 1 \quad \text{and} \quad -\tilde{X}_{j,t} \leq 0$$

each contribute an identity matrix in the columns corresponding to the variables $\tilde{X}_{j,t}$, while

$$\tilde{\delta}_{j,t} \leq 1 \quad \text{and} \quad -\tilde{\delta}_{j,t} \leq 0$$

each contribute an identity matrix in the columns corresponding to the variables $\tilde{\delta}_{j,t}$. Appending rows corresponding to identity matrices (or their negations) above or below an existing constraint matrix preserves total unimodularity. Therefore, the full constraint matrix associated with (C1), together with the variable bound constraints, is totally unimodular. Since the right-hand-side vector is integral, it follows that every vertex of R is integral, and hence R is an integral polyhedron. \square

Proposition 3 (Non-Integrality of the (B1) Polyhedron). *Let S denote the polyhedron defined by the constraint set (B1), i.e., constraints (2.2.1)–(2.2.4), together with the relaxed bounds on the segment-assignment variables*

$$\tilde{\delta}_{j,t} \in [0, 1], \quad \forall j = 1, \dots, K, t = 1, \dots, T.$$

Then the polyhedron S is not integral.

Proof. We show that the polyhedron S admits fractional extreme points for general values of K . An explicit example is provided in Appendix A.4, where we provide a fractional corner point, and prove that it is indeed a corner point. \square

We summarize the key insights from the analysis in this section as follows. Proposition 1 shows that replacing the Basic segment-assignment block (A1) by the extended block (C1) yields a strictly tighter LP relaxation in the shared δ -variable space; specifically, the projection of the Extended Basic relaxation is a strict subset of the projection of the Basic relaxation. Proposition 2 establishes that the polyhedron defined by (C1), together with relaxed binary bounds, is integral, implying that the associated segment-assignment variables admit integral extreme points under LP relaxation. In contrast, Proposition 3 shows that the alternate segment-assignment block (B1), together with relaxed binary bounds, defines a non-integral polyhedron and can therefore admit fractional extreme points and nonzero integrality gaps. Taken together, these results indicate that, from the standpoint of the segment-assignment variables and constraints, the extended block (C1) excludes certain fractional segment-assignment patterns (as illustrated in Figure 3) while defining an integral polyhedron. This polyhedral strengthening provides a mechanism by which the extended formulations can tighten the root LP relaxation and reduce the amount of branch-and-bound exploration required to enforce integrality on the segment assignment variables. We emphasize, however, that the above propositions focus either on projections onto the δ -variable space or on polyhedra formed by subsets of constraints related to partitioning the data into contiguous segments. While these analyses provide insight into potential differences in LP relaxation strength and convergence behavior, the full MIP formulations also differ in how slopes and intercepts are assigned to each segment in the piecewise linear fitting problem. As a result, the polyhedral comparisons in this section are not conclusive with respect to overall computational performance, which is therefore assessed empirically in Section 5.

4 Multidimensional and Sparse Change-Point Detection

We adapt the Basic, Alternate and Extended MIP formulations discussed in Section 2 for multidimensional change-point detection, in which all response components share a common set of breakpoints and are fit with separate piecewise-linear functions over these segments for each dimension. We then further modify these formulations to a sparse change-point detection setting, in which only a subset of dimensions is allowed to undergo a structural change at any given shared breakpoint. As is consistent with the change-point detection literature, we do not enforce continuity constraints in these settings.

4.1 Multidimensional Change-point detection

We consider observations

$$\{(x_t, \mathbf{y}_t)\}_{t=1}^T,$$

where $x_t \in \mathbb{R}$ and $\mathbf{y}_t = (y_t^1, \dots, y_t^D)^\top \in \mathbb{R}^D$. As in the univariate case, we restrict attention to a univariate input domain and seek to fit D piecewise-linear functions that share a common set of breakpoints. For each response dimension $d \in \{1, \dots, D\}$, we consider a fitted function of the form

$$f^d(x \mid \boldsymbol{\theta}^d) = \begin{cases} m_1^d x + c_1^d, & x \in [r_0, r_1], \\ m_2^d x + c_2^d, & x \in (r_1, r_2], \\ \vdots \\ m_{K-1}^d x + c_{K-1}^d, & x \in (r_{K-2}, r_{K-1}], \\ m_K^d x + c_K^d, & x \in (r_{K-1}, r_K], \end{cases}$$

where the dimension-specific parameter vector

$$\boldsymbol{\theta}^d = (\{m_i^d, c_i^d\}_{i=1}^K, r_0, r_1, \dots, r_K)$$

collects the slopes and intercepts for response d , together with the shared breakpoint locations. Each $\boldsymbol{\theta}^d$ is assumed to belong to a parameter space $\boldsymbol{\Theta}^d$ that imposes bounds on (m_i^d, c_i^d) consistent with the observed data as defined for the univariate setting. Let $\hat{y}_t^d := f^d(x_t \mid \boldsymbol{\theta}^d)$ denote the fitted value for component d at index t . For $q \in \{1, 2\}$, the multidimensional fitting problem is then formulated as

$$\min_{\{\boldsymbol{\theta}^d\}_{d=1}^D} \sum_{d=1}^D \sum_{t=1}^T |y_t^d - \hat{y}_t^d|^q,$$

subject to $\boldsymbol{\theta}^d \in \boldsymbol{\Theta}^d$ for all $d = 1, \dots, D$, and with a common set of breakpoints (r_0, \dots, r_K) shared across all dimensions. The multidimensional extension replicates the univariate PWL fitting parameters and error variables across dimensions, while sharing the segment assignment variables. For all $j \in \{1, \dots, K\}$, $t \in \{1, \dots, T\}$, and $d \in \{1, \dots, D\}$, the value-assignment constraints become

$$\begin{aligned} m_j^d x_t + c_j^d &\leq \hat{y}_t^d + M_{1,t}^{A,d} (1 - \delta_{j,t}) \\ m_j^d x_t + c_j^d &\geq \hat{y}_t^d - M_{1,t}^{A,d} (1 - \delta_{j,t}) \end{aligned}$$

where $\delta_{j,t}$ is common across all d and thus enforces a shared segmentation. The slope and intercept bounds are imposed dimension-wise. The derivation of the Big- M constants and parameter bounds is performed separately for each dimension, using the same methodology as in the univariate setting as discussed in Appendix A.1.

$$m_j^d \in [L_d^m, U_d^m], \quad c_j^d \in [L_d^c, U_d^c], \quad j = 1, \dots, K, \quad d = 1, \dots, D,$$

4.2 Sparse Change-point Detection

The multidimensional formulation above enforces a common breakpoint structure across all D response dimensions. In many applications, however, structural changes occur only in a subset of dimensions, while the remaining series remain unchanged. We capture this behavior through sparse change-point detection. In this setting, we restrict our attention to the case where exactly one shared breakpoint is allowed, and only a limited number of dimensions may undergo a structural change at this breakpoint. The aim of our proposed MIP is to select the dimensions that undergo a change in their linear parameters and minimize a chosen error norm for the overall fit obtained. To model this, we introduce binary indicator variables $\eta_d \in \{0, 1\}$ for $d = 1, \dots, D$, where $\eta_d = 1$ indicates that dimension d undergoes a structural change at r , and $\eta_d = 0$ otherwise. Structural

change may manifest as a change in slope, a change in intercept, or both. We control changes in slopes and intercepts separately using the following Big- M constraints:

$$-(M_d^m) \eta_d \leq m_2^d - m_1^d \leq (M_d^m) \eta_d, \quad d = 1, \dots, D, \quad (4.2.1)$$

$$-(M_d^c) \eta_d \leq c_2^d - c_1^d \leq (M_d^c) \eta_d, \quad d = 1, \dots, D. \quad (4.2.2)$$

Here, M_d^m and M_d^c are sufficiently large constants bounding admissible slope and intercept changes for each dimension d , as given by:

$$M_d^m = U_d^m - L_d^m, \quad (4.2.3)$$

$$M_d^c = U_d^c - L_d^c. \quad (4.2.4)$$

These are used to activate or deactivate dimension-specific change-points using the binary indicators η_d . When $\eta_d = 0$ (i.e., deactivating the existence of a change in dimension d), constraints (4.2.1)–(4.2.2) enforce $m_2^d = m_1^d$ and $c_2^d = c_1^d$, thereby ruling out any structural change in dimension d . Sparsity is enforced through the cardinality constraint

$$\sum_{d=1}^D \eta_d \leq S, \quad (4.2.5)$$

where S is an inputted upper bound on the number of dimensions permitted to undergo a structural change. Together, constraints (4.2.1)–(4.2.5) enable sparse detection of structural changes—encompassing slope changes, intercept shifts, or both under a shared breakpoint structure.

5 Experiments

We conduct computational experiments to compare the relative runtime performance of the proposed extended segment-assignment constraint formulation against the existing segment-assignment formulations, namely the Basic and Alternate formulations. These experiments complement and further substantiate the theoretical analysis provided in Section 3. All experiments were conducted using Gurobi Optimizer 12.0.3 on an Apple M3 processor with eight physical cores and eight logical processors, using up to eight threads. A wall-clock time limit of 2000 seconds was imposed for every run, and non-default parameters were kept minimal to avoid solver-specific tuning effects. This standardized setup ensures an equitable comparison across formulations and aims to reflect differences arising purely from modeling strength.

5.1 Experiments: Univariate sequence with continuity

The Basic, Alternate, and Extended formulations each contain a block of segment-assignment constraints. In addition, the Basic and Alternate formulations differ in the manner in which continuity between segments is enforced. Since the extended segment-assignment constraint block is modular and can be combined with either of these continuity-enforcing constraint blocks, this naturally leads to a comparison of four MIP formulations for change-point detection via piecewise linear fitting with continuity, namely the benchmark formulations (Basic and Alternate) and their extended counterparts (Extended Basic and Extended Alternate). We perform a computational analysis comparing the runtimes of these formulations across a wide range of time-series lengths (i.e., T), segmentation levels (i.e., K), and error norms (i.e., ℓ_1 - and ℓ_2 -error norms), thereby providing a comprehensive view of solver performance under diverse modeling regimes. We use financial time

series obtained through the `yfinance` Python library. Specifically, we analyze daily closing prices for five major publicly traded companies: Apple Inc. (AAPL), Microsoft Corporation (MSFT), Amazon.com Inc. (AMZN), Alphabet Inc. (GOOGL), and Johnson & Johnson (JNJ). The starting date for each financial time series is taken to be January 1, 2015. For each company, we consider time-series lengths

$$T \in \{100, 200, 300, 400, 500\},$$

which correspond to the first T entries in the time series, and for each instance, we fit models using

$$K \in \{2, 3, 4, 5\} \text{ segments.}$$

This setup results in 200 distinct experimental settings, each defined by a specific company, time horizon, number of segments, and error norm. The design of our computational experiments is inspired by existing studies such as Rebennack and Krasko [2020].

5.2 Experiments: Univariate sequence without continuity

The comparison under the non-continuous setting focuses solely on the computational performance of the segment-assignment constraint blocks across the MIP formulations. Accordingly, in this setting, as well as in the remaining settings, namely multidimensional change-point detection (Section 5.3) and sparse change-point detection (Section 5.4), we perform a comparison among three MIP formulations, corresponding to the Basic, Alternate, and Extended segment assignment constraint blocks. We compare these formulations by fitting daily closing price data for Apple Inc. (AAPL), Microsoft Corporation (MSFT), Amazon.com Inc. (AMZN), and Alphabet Inc. (GOOGL). The starting date for each financial time series is taken to be January 1, 2015. For each company, we consider time-series lengths

$$T \in \{100, 200, 300, 400, 500\},$$

and for each instance, we fit models using

$$K \in \{2, 3, 4, 5, 6\} \text{ segments.}$$

Here, we include one additional level of segmentation (i.e., $K = 6$), as removing the continuity constraints improves the scalability of the MIP and enables convergence to global optimality within the prescribed runtime limit. This setup results in 200 distinct experimental settings.

5.3 Experiments: Multidimensional change-point detection

We evaluate the computational performance of the proposed multidimensional change-point detection formulations using daily closing price data for the following publicly traded companies, namely Apple Inc. (AAPL), Microsoft Corporation (MSFT), Amazon.com Inc. (AMZN), Alphabet Inc. (GOOGL), Meta Platforms, Inc. (META), Tesla, Inc. (TSLA), NVIDIA Corporation (NVDA), JPMorgan Chase & Co. (JPM), Berkshire Hathaway Inc. Class B (BRK-B), and Johnson & Johnson (JNJ), covering the period from January 1, 2015 to December 31, 2024. To construct a D -dimensional signal, we select the first D tickers from this list and jointly fit their price trajectories using the proposed multidimensional formulation. We consider dimensionalities

$$D \in \{2, 4, 6, 8, 10\},$$

time-series lengths

$$T \in \{100, 200, 300, 400, 500\},$$

and segmentations corresponding to

$$K \in \{2, 3, 4, 5\},$$

yielding a total of 200 distinct experimental configurations.

5.4 Experiments: Sparse change-point detection

We evaluate the computational performance of the proposed sparse change-point detection formulations using daily closing price data for a fixed set of large-cap U.S. equities, observed over the period January 1, 2015 to December 31, 2024. To construct a D -dimensional signal, we select the first D stocks from a fixed ordering of tickers (listed in Appendix A.8) and jointly model their price trajectories using the proposed sparse change-point detection formulation. We consider

$$D \in \{10, 20, 30, 40\},$$

and truncate each series to the first $T = 200$ observations. For each dimensionality D , we impose a cardinality constraint that limits the number of dimension-specific fittings permitted to undergo a structural change, specified as a fixed fraction (10%, 20%, or 30%) of D . This results in a total of 24 experimental settings. Since the MIP formulations become increasingly difficult to scale with larger dimensions, we restrict our computational experiments to this limited set of configurations, in contrast to the broader settings considered in the preceding experimental sections.

6 Results

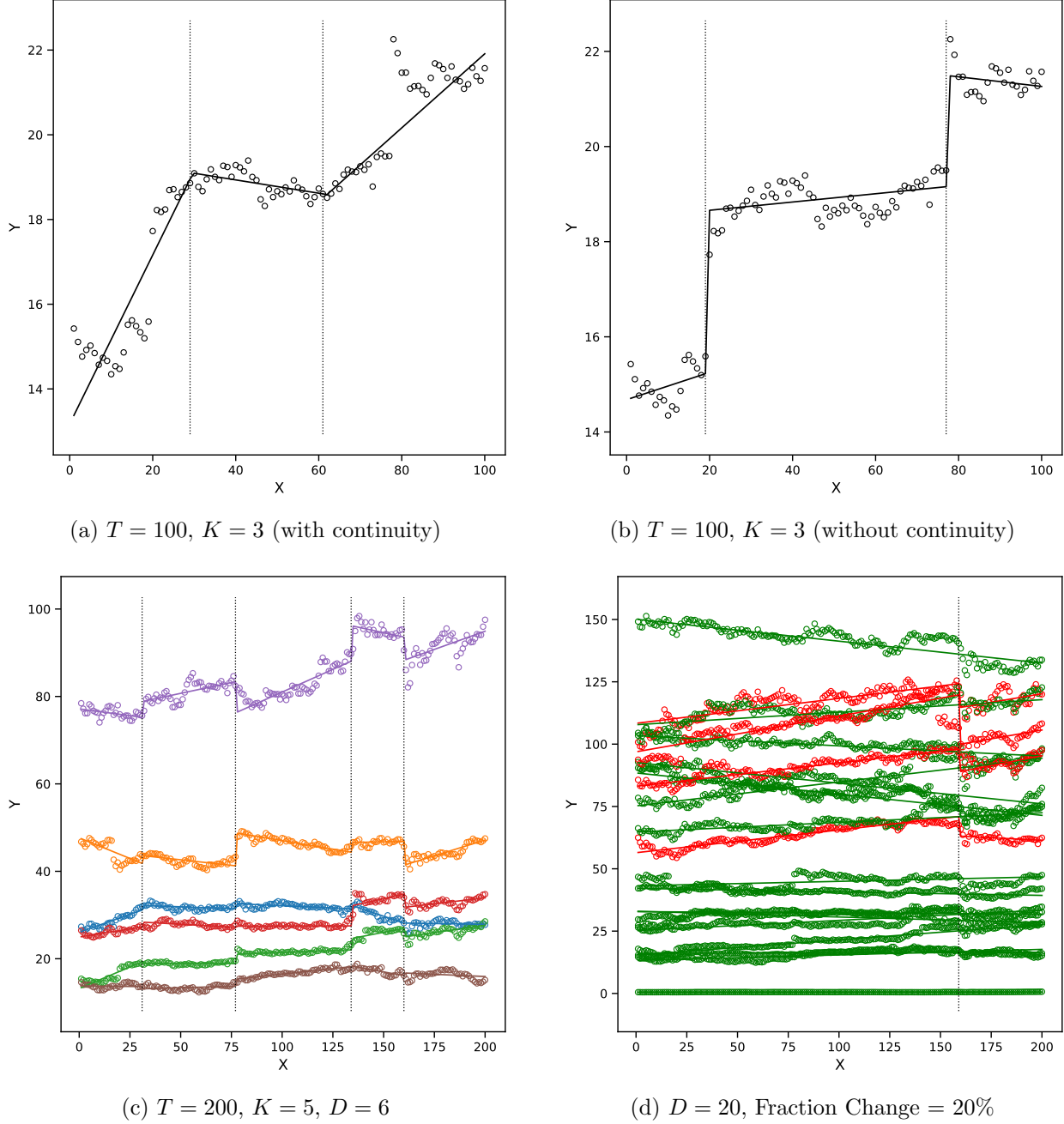


Figure 4: Illustration of piecewise-linear (PWL) fits obtained through MIP-based offline change-point detection under different modeling regimes. (a) Univariate PWL fit with continuity constraints, using $K = 3$ linear segments to model a length- $T = 100$ time series of daily closing prices for Amazon (AMZN). (b) Univariate PWL fit without continuity constraints for the same data and number of segments. (c) Multidimensional change-point detection with a shared set of change-points across $D = 6$ dimensions, using $K = 5$ linear segments to jointly fit all series. (d) Sparse change-point detection in a $D = 20$ -dimensional setting with a sparsity level of 20%, allowing 4 out of 20 dimensions to undergo a change in their fitted parameters.

Table 1: Summary of runtime performance across all computational experiments. Each entry reports the number of instances in which a formulation converged fastest to the global optimum. When all formulations reached the 2000-second time limit on an instance, the comparison is based on the final integrality gap.

Experiment Class	Setting	Norm	Basic	Alternate	Extended	Total
Single-Dimensional PWL Fitting	Without Continuity	ℓ_1	5	41	54	100
		ℓ_2	4	27	69	100
	With Continuity	ℓ_1	25	8	67	100
		ℓ_2	4	36	60	100
Multi-Dimensional PWL Fitting		ℓ_1	8	46	46	100
		ℓ_2	17	40	43	100
Sparse Change-Point Detection		ℓ_1	2	4	6	12
		ℓ_2	7	4	1	12
Overall Total (All Settings)			72	206	346	624

Note. For Single-Dimensional PWL Fitting with Continuity, the Extended column aggregates results from two variants. For the ℓ_1 norm, Extended Basic is fastest in 44 instances and Extended Alternate in 23 instances. For the ℓ_2 norm, the corresponding counts are 11 and 49.

Tables 1 and 2 provide a unified view of solver performance across all experiment classes and settings. As summarized in Table 1, the Extended formulations achieve the fastest convergence in the majority of instances overall (346 out of 624), outperforming both Basic (72/624) and Alternate (206/624). This advantage is particularly pronounced in the single-dimensional setting (both with and without continuity) and persists in the multi-dimensional shared-breakpoint experiments, indicating that the proposed strengthening translates into consistently improved computational behavior across modeling regimes. Complementing this instance-wise summary, Table 2 shows that Extended formulations also yield the lowest cumulative runtime across all settings (75,538.042 seconds, versus 89,538.370 for Alternate and 118,593.459 for Basic), with the largest gains occurring in the continuity-constrained univariate benchmarks where many hard instances approach the 2000s time limit. These aggregate summaries are obtained by consolidating the detailed per-instance runtimes and integrality gaps reported in Appendix Tables 3 (univariate without continuity), 4 (univariate with continuity), 5 (multi-dimensional shared change-points), and 6 (sparse change-point detection). Figure 4 visually illustrates representative fits from each regime, namely univariate with and without continuity (Figures 4a - 4b), multi-dimensional fitting with shared change-points (Figure 4c), and sparse change-point detection (Figure 4d), corresponding to the same experimental settings whose computational outcomes are summarized in Tables 1 and 2.

Table 2: Unified comparison of total runtime across all computational experiments. Entries report the cumulative solver time (in seconds) required to complete all instances for each setting and formulation. Instances that reached the runtime limit are counted as having runtime 2000 seconds.

Experiment Class	Setting	Norm	Basic	Alternate	Extended
Single-Dimensional PWL Fitting	Without Continuity	ℓ_1	3023.875	2632.636	3552.875
		ℓ_2	1046.199	661.496	566.400
	With Continuity	ℓ_1	41452.293	35516.638	24351.855
		ℓ_2	48775.096	23839.948	21994.230
Multi-Dimensional PWL Fitting		ℓ_1	8112.499	8833.510	7759.762
		ℓ_2	3576.805	3435.832	3574.148
Sparse Change-Point Detection		ℓ_1	3046.154	3882.812	3358.677
		ℓ_2	9560.538	10735.498	10380.095
Overall Total (All Settings)			118593.459	89538.370	75538.042

7 Conclusion

This work addresses the statistical problem of change-point detection under various settings, including multiple change-point detection in the univariate case, multidimensional change-point detection, and sparse change-point detection, through a unified MIP-based framework for piecewise-linear fitting. The key contribution is a novel set of constraints for partitioning the data into contiguous segments, where each segment is fit by a linear function. These constraints exhibit favorable theoretical properties that contribute to faster solver runtimes. In particular, relaxing the integrality requirements on the segment-assignment variables yields LP relaxations whose feasible region forms an integral polytope. We provide theoretical arguments to explain why the proposed segment-assignment constraints lead to improved computational performance and complement these results with comprehensive computational experiments that empirically verify the claimed improvements. Promising avenues for future research include enhancing scalability through decomposition techniques for sparse change-point detection and developing online variants of the proposed change-point detection framework.

Acknowledgments

The work of Narula and Xie is partially supported by National Science Foundation DMS-2220495.

References

Hamed Ahmadi, José R Martí, and Ali Moshref. Piecewise linear approximation of generators cost functions using max-affine functions. In *2013 IEEE Power & Energy Society General Meeting*, pages 1–5. IEEE, 2013.

Dimitris Bertsimas and Romy Shioda. Classification and regression via integer optimization. *Operations research*, 55(2):252–271, 2007.

Papraphee Buason, Sidhant Misra, and Daniel K Molzahn. Sample-based piecewise linear power flow approximations using second-order sensitivities. *arXiv preprint arXiv:2501.13825*, 2025.

Yang Cao, Yao Xie, and Nagi Gebraeel. Multi-sensor slope change detection. *Annals of Operations Research*, 263(1):163–189, 2018.

Ying Cui, Jong-Shi Pang, and Bodhisattva Sen. Composite difference-max programs for modern statistical estimation problems. *SIAM Journal on Optimization*, 28(4):3344–3374, 2018.

Jonas Dehning, Johannes Zierenberg, F Paul Spitzner, Michael Wibral, Joao Pinheiro Neto, Michael Wilczek, and Viola Priesemann. Inferring change points in the spread of covid-19 reveals the effectiveness of interventions. *Science*, 369(6500):eabb9789, 2020.

Xiaoyong Gao, Zhenhui Feng, Yuhong Wang, Xiaolin Huang, Dexian Huang, Tao Chen, and Xue Lian. Piecewise linear approximation based milp method for pvc plant planning optimization. *Industrial & Engineering Chemistry Research*, 57(4):1233–1244, 2018.

Noam Goldberg, Steffen Rebennack, Youngdae Kim, Vitaliy Krasko, and Sven Leyffer. Minlp formulations for continuous piecewise linear function fitting. *Computational Optimization and Applications*, 79(1):223–233, 2021.

Zaid Harchaoui and Céline Lévy-Leduc. Multiple change-point estimation with a total variation penalty. *Journal of the American Statistical Association*, 105(492):1480–1493, 2010.

Lingxun Kong and Christos T Maravelias. On the derivation of continuous piecewise linear approximating functions. *INFORMS Journal on Computing*, 32(3):531–546, 2020.

Quentin Ploussard. Piecewise linear approximation with minimum number of linear segments and minimum error: A fast approach to tighten and warm start the hierarchical mixed integer formulation. *European Journal of Operational Research*, 315(1):50–62, 2024.

Artem Prokhorov, Peter Radchenko, Alexander Semenov, and Anton Skrobotov. Change-point detection in time series using mixed integer programming. *Journal of Business & Economic Statistics*, (just-accepted):1–24, 2025.

Steffen Rebennack and Vitaliy Krasko. Piecewise linear function fitting via mixed-integer linear programming. *INFORMS Journal on Computing*, 32(2):507–530, 2020.

Joanna Tobiasz, Najla Al-Harbi, Sara Bin Judia, Salma Majid Wakil, Joanna Polanska, and Ghazi Alsbeih. Multivariate piecewise linear regression model to predict radiosensitivity using the association with the genome-wide copy number variation. *Frontiers in Oncology*, 13:1154222, 2023.

Alejandro Toriello and Juan Pablo Vielma. Fitting piecewise linear continuous functions. *European Journal of Operational Research*, 219(1):86–95, 2012.

Anita K Wagner, Stephen B Soumerai, Fang Zhang, and Dennis Ross-Degnan. Segmented regression analysis of interrupted time series studies in medication use research. *Journal of clinical pharmacy and therapeutics*, 27(4):299–309, 2002.

Tengyao Wang and Richard J Samworth. High dimensional change point estimation via sparse projection. *Journal of the Royal Statistical Society Series B: Statistical Methodology*, 80(1):57–83, 2018.

John Alasdair Warwicker and Steffen Rebennack. A comparison of two mixed-integer linear programs for piecewise linear function fitting. *INFORMS journal on computing*, 34(2):1042–1047, 2022.

John Alasdair Warwicker and Steffen Rebennack. A unified framework for bivariate clustering and regression problems via mixed-integer linear programming. *Discrete Applied Mathematics*, 336: 15–36, 2023.

Yao Xie and David Siegmund. Sequential multi-sensor change-point detection. In *2013 Information theory and applications workshop (ITA)*, pages 1–20. IEEE, 2013.

Nancy R Zhang and David O Siegmund. A modified bayes information criterion with applications to the analysis of comparative genomic hybridization data. *Biometrics*, 63(1):22–32, 2007.

Appendix

A.1 Choice of Big- M Constants for PWL Fitting

This section derives a data-driven parameter space Θ for $\theta = (\{m_i, c_i\}_{i=1}^K, r_0, \dots, r_K)$ and derives valid Big- M constants for the one-dimensional PWL formulations in Sections 2.1 and 2.2. Assuming the inputs satisfy $x_1 < x_2 < \dots < x_T$, we define the global slope bounds induced by the data as

$$L^m := \min_{\substack{t_1, t_2 \in \{1, \dots, T\} \\ t_1 \neq t_2}} \frac{y_{t_1} - y_{t_2}}{x_{t_1} - x_{t_2}}, \quad (\text{A.1.1})$$

$$U^m := \max_{\substack{t_1, t_2 \in \{1, \dots, T\} \\ t_1 \neq t_2}} \frac{y_{t_1} - y_{t_2}}{x_{t_1} - x_{t_2}}. \quad (\text{A.1.2})$$

These bounds are valid for the slope of any linear segment that fits the data over a sub-interval of the observed domain. Given L^m and U^m , we define intercept bounds by requiring that each linear function $mx + c$ can attain observed values over the domain $\{x_t\}_{t=1}^T$:

$$L^c := \min_{t \in \{1, \dots, T\}} \min\{y_t - L^m x_t, y_t - U^m x_t\}, \quad (\text{A.1.3})$$

$$U^c := \max_{t \in \{1, \dots, T\}} \max\{y_t - L^m x_t, y_t - U^m x_t\}. \quad (\text{A.1.4})$$

The breakpoint bounds are obtained based on the convention that $r_0 = x_1$ and $r_K = x_T$. We restrict all interior breakpoints to $[x_1, x_T]$ and impose strict ordering:

$$x_1 = r_0 \leq r_1 \leq \dots \leq r_{K-1} \leq r_K = x_T, \quad r_j \in [x_1, x_T] \quad \forall j = 1, \dots, K-1. \quad (\text{A.1.5})$$

We therefore define the parameter space:

$$\Theta := \left\{ \theta = (\{m_i, c_i\}_{i=1}^K, r_0, \dots, r_K) : m_i \in [L^m, U^m], c_i \in [L^c, U^c] \quad \forall i, \text{ and (A.1.5) holds} \right\}. \quad (\text{A.1.6})$$

We use the above bounds to derive valid Big- M constants for the value-assignment and breakpoint-localization constraints in (2.1.2)–(2.1.3) and (2.1.4)–(2.1.5), respectively. To ensure a fair and consistent comparison across MIP benchmarks, we adopt the same Big- M construction as in Rebennack and Krasko [2020]. For the value-assignment constraints (2.1.2)–(2.1.3), the constant $M_{1,t}^A$ must dominate the fitted value at x_t whenever $\delta_{j,t} = 0$, and is obtained as:

$$M_{1,t}^A = \max \left\{ |L^m x_t| + |L^c|, |U^m x_t| + |L^c|, |L^m x_t| + |U^c|, |U^m x_t| + |U^c| \right\}, \quad t = 1, \dots, T. \quad (\text{A.1.7})$$

For the breakpoint-localization constraints (2.1.4)–(2.1.5), note that $x_1 \leq r_j \leq x_T$ for all breakpoints r_j , and $x_1 \leq x_t \leq x_T$ for all t . It is therefore sufficient to choose:

$$M_{2,t}^A = x_t - x_1, \quad (\text{A.1.8})$$

$$M_{3,t}^A = x_T - x_t, \quad (\text{A.1.9})$$

which ensures that the corresponding inequalities are automatically satisfied whenever $\delta_{j,t} = 0$. Finally, the linearized continuity constraints (2.2.5)–(2.2.8) require a Big- M constant $M_{4,t}^B$ that dominates expressions of the form $|x_t(m_j - m_{j+1}) - (c_{j+1} - c_j)|$. Over $(m_j, m_{j+1}) \in [L^m, U^m]^2$ and $(c_j, c_{j+1}) \in [L^c, U^c]^2$, we have $|m_j - m_{j+1}| \leq U^m - L^m$ and $|c_{j+1} - c_j| \leq U^c - L^c$. Hence, we obtain:

$$M_{4,t}^B = |x_t| (U^m - L^m) + (U^c - L^c), \quad t = 1, \dots, T. \quad (\text{A.1.10})$$

A.2 MIP for PWL Fitting with ℓ_0 Regularization

As discussed in Section 2, the Basic and Extended Basic formulations allow the parameter K to act as an upper bound on the number of linear segments. Consequently, these formulations can be naturally adapted to perform piecewise-linear (PWL) fitting with ℓ_0 regularization on the number of segments. To enable ℓ_0 regularization, we explicitly count the number of segments that are activated in the model. This is achieved by introducing an auxiliary binary variable δ_j^R for each segment $j = 1, \dots, K$, which indicates whether segment j is used. The following constraint block is added to the formulation:

(R1) Segment usage indicator constraints:

$$\sum_{t=1}^T \delta_{j,t} \leq M^R (1 - \delta_j^R), \quad \forall j = 1, \dots, K. \quad (\text{A.2.1})$$

Here, M^R is a sufficiently large constant. Since $\delta_{j,t} \in \{0, 1\}$ for all t , a valid choice is $M^R = T$, as $\sum_{t=1}^T \delta_{j,t} \leq T$ holds trivially. Constraint (A.2.1) enforces $\delta_j^R = 1$ whenever segment j is used by at least one data point, and allows $\delta_j^R = 0$ only when the segment is entirely inactive.

Objective function With these additional variables, the objective function is modified to penalize the number of active segments:

$$\min \sum_{t=1}^T |y_t - \hat{y}_t|^q + \lambda_0 \sum_{j=1}^K \delta_j^R, \quad q \in \{1, 2\}. \quad (\text{A.2.2})$$

Here, $\lambda_0 > 0$ is a regularization parameter that controls the trade-off between goodness of fit and model complexity, and can be selected based on the dataset or by cross-validation.

A.3 LP Relaxation: Feasible Construction Supporting Proposition 1

We show that it is possible to construct a feasible solution that satisfies the breakpoint localization constraints (2.1.4), (2.1.5), (2.1.6), and (2.1.7). All remaining constraints of the Basic formulation are trivially satisfiable. We therefore focus on explicitly constructing the breakpoint variables $\{r_j\}$ that support a feasible LP-relaxed segment assignment. Considering the instance discussed in

Proposition 1 with $T = 8$ data points $\{x_t\}_{t=1}^T$ and $K = 4$ segments. This consists of the LP-relaxed segment-assignment variables as follows:

$$\begin{aligned}\tilde{\delta}_{1,\cdot} &= [0.5, 0.5, 0.5, 0.5, 0.5, 0.5, 0.5, 0.5], \\ \tilde{\delta}_{2,\cdot} &= [0.4, 0.1, 0.4, 0.1, 0.4, 0.1, 0.4, 0.1], \\ \tilde{\delta}_{3,\cdot} &= [0.1, 0.4, 0.1, 0.4, 0.1, 0.4, 0.1, 0.4], \\ \tilde{\delta}_{4,\cdot} &= [0, 0, 0, 0, 0, 0, 0, 0].\end{aligned}$$

The big- M constants in constraints (2.1.5) and (2.1.4) are given by

$$M_{2,t}^A = x_t - x_1, \quad M_{3,t}^A = x_8 - x_t.$$

Since this is a $K = 4$ segment example, we construct $K + 1 = 5$ breakpoints as follows:

$$r_0 = x_1, \quad r_1 = r_2 = r_3 = \frac{x_1 + x_8}{2}, \quad r_4 = x_8.$$

We now verify feasibility with respect to constraints (2.1.5) and (2.1.4) for each segment.

Segment $j = 1$. For $\tilde{\delta}_{1,t} = 0.5$ for all t , constraint (2.1.5) requires

$$x_t - r_1 \leq M_{2,t}^A(1 - \tilde{\delta}_{1,t}) = \frac{x_t - x_1}{2}.$$

This implies

$$x_t - \frac{x_t - x_1}{2} \leq r_1 \iff \frac{x_t + x_1}{2} \leq r_1,$$

which is satisfied for all t by the choice $r_1 = \frac{x_1 + x_8}{2}$.

Constraint (2.1.4) is always satisfied since

$$r_0 - x_t = x_1 - x_t \leq 0 \leq M_{3,t}^A(1 - \tilde{\delta}_{1,t}).$$

Segments $j = 2, 3$. For $j \in \{2, 3\}$, we have $\tilde{\delta}_{j,t} \in \{0.1, 0.4\}$ and $r_j = r_{j-1} = \frac{x_1 + x_8}{2}$. Constraint (2.1.5) requires

$$x_t - r_j = x_t - \frac{x_1 + x_8}{2} \leq \frac{x_t - x_1}{2} \leq 0.6(x_t - x_1) = M_{2,t}^A(1 - \tilde{\delta}_{j,t}),$$

which holds since $1 - \tilde{\delta}_{j,t} \geq 0.6$.

To verify constraint (2.1.4), we observe that

$$r_{j-1} - x_t = \frac{x_1 + x_8}{2} - x_t.$$

We define $\tilde{x}_t := x_t - x_1$ and $\tilde{x}_T := x_T - x_1$. Then

$$r_{j-1} - x_t = \frac{\tilde{x}_T - \tilde{x}_t}{2} \leq 0.6(\tilde{x}_T - \tilde{x}_t) = 0.6(x_T - x_t) \leq M_{3,t}^A(1 - \tilde{\delta}_{j,t}),$$

where the inequality holds since $\tilde{x}_t, \tilde{x}_T \geq 0$ and $1 - \tilde{\delta}_{j,t} \geq 0.6$.

Segment $j = 4$. For the final segment, $\tilde{\delta}_{4,t} = 0$ for all t . Hence, constraints (2.1.5) and (2.1.4) reduce to

$$x_t - r_4 \leq M_{2,t}^A, \quad r_3 - x_t \leq M_{3,t}^A,$$

both of which are trivially satisfied by construction. This completes the feasible LP-relaxed construction supporting Proposition 1.

A.4 Fractional Corner Point Supporting Proposition 3

We consider an instance with $T = 6$ data points and $K = 4$ candidate segments. For this setting, we construct the following fractional point, which we show to be a corner point of the polyhedron S defined in Proposition 3. The segment-assignment variables are given by

$$\begin{aligned}\tilde{\delta}_{1,\cdot} &= [0.5, 0.5, 0.5, 0, 0, 0], \\ \tilde{\delta}_{2,\cdot} &= [0, 0.5, 0, 0.5, 0.5, 0.5], \\ \tilde{\delta}_{3,\cdot} &= [0.5, 0, 0.5, 0, 0, 0], \\ \tilde{\delta}_{4,\cdot} &= [0, 0, 0, 0.5, 0.5, 0.5].\end{aligned}$$

It is straightforward to verify that this point is feasible for S , as it satisfies all assignment, contiguity, and boundary constraints. To establish that this point is an corner point of S , we identify 24 linearly independent constraints that are tight at this point. Since the ambient space is \mathbb{R}^{24} (corresponding to the variables $\{\tilde{\delta}_{j,t}\}_{j=1,\dots,4; t=1,\dots,6}$), this suffices for the proof.

Tight constraints

1. **Assignment constraints.** There are 6 equality constraints of type (2.2.1):

$$\sum_{j=1}^4 \tilde{\delta}_{j,t} = 1, \quad \forall t = 1, \dots, 6.$$

2. **Contiguity constraints.** The following 6 constraints of type (2.2.2) are tight:

$$\begin{aligned}\tilde{\delta}_{2,2} &= \tilde{\delta}_{1,1} + \tilde{\delta}_{2,1}, \\ \tilde{\delta}_{2,4} &= \tilde{\delta}_{1,3} + \tilde{\delta}_{2,3}, \\ \tilde{\delta}_{2,5} &= \tilde{\delta}_{1,4} + \tilde{\delta}_{2,4}, \\ \tilde{\delta}_{2,6} &= \tilde{\delta}_{1,5} + \tilde{\delta}_{2,5}, \\ \tilde{\delta}_{3,3} &= \tilde{\delta}_{2,2} + \tilde{\delta}_{3,2}, \\ \tilde{\delta}_{4,4} &= \tilde{\delta}_{4,3} + \tilde{\delta}_{3,3},\end{aligned}$$

3. **Boundary constraints.** There are 4 tight constraints of types (2.2.3)–(2.2.4):

$$\begin{aligned}\tilde{\delta}_{1,1} &= \tilde{\delta}_{1,2}, & \tilde{\delta}_{1,2} &= \tilde{\delta}_{1,3}, \\ \tilde{\delta}_{4,4} &= \tilde{\delta}_{4,5}, & \tilde{\delta}_{4,5} &= \tilde{\delta}_{4,6}.\end{aligned}$$

4. **Variable bound constraints.** Finally, the following 8 variable bounds are tight:

$$\tilde{\delta}_{1,5} = 0, \quad \tilde{\delta}_{1,6} = 0, \quad \tilde{\delta}_{2,1} = 0, \quad \tilde{\delta}_{2,3} = 0, \quad \tilde{\delta}_{3,2} = 0, \quad \tilde{\delta}_{3,5} = 0, \quad \tilde{\delta}_{4,1} = 0, \quad \tilde{\delta}_{4,3} = 0.$$

Together, these 24 linearly independent tight constraints uniquely determine the point, thereby proving that it is an extreme point of S . Since this extreme point is fractional, the polyhedron S is not integral, completing the proof of Proposition 3.

A.5 Computational Results for Univariate Piecewise Linear Fitting without Continuity

Table 3: Comparison of runtimes (in seconds) for the Basic, Alternate, and Extended formulations for univariate non-continuous PWL fitting. Results corresponding to ℓ_1 and ℓ_2 losses are reported sequentially. Bold entries mark the fastest formulation, and bracketed values denote integrality gaps when the 2000 s time limit is reached.

T	Basic					Alternate					Extended				
	K=2	K=3	K=4	K=5	K=6	K=2	K=3	K=4	K=5	K=6	K=2	K=3	K=4	K=5	K=6
ℓ_1 norm															
AAPL															
100	0.104	0.395	0.915	2.814	12.918	0.054	0.240	0.578	3.325	12.306	0.052	0.171	0.437	3.316	13.610
200	0.342	0.689	2.086	27.932	88.491	0.183	0.608	1.285	12.512	181.119	0.159	0.493	1.802	12.312	101.547
300	0.622	1.304	3.901	24.858	155.869	0.386	0.807	3.250	16.888	168.853	0.346	0.731	2.507	15.903	137.824
400	0.828	2.130	8.487	28.721	129.915	0.377	1.423	5.744	39.795	246.895	0.572	1.039	4.131	21.903	141.243
500	0.909	3.819	13.804	45.819	255.298	0.567	1.968	13.029	33.339	260.044	0.503	1.312	6.553	30.322	406.932
AMZN															
100	0.116	0.317	0.507	1.291	5.891	0.054	0.211	0.419	0.778	3.810	0.061	0.164	0.332	0.641	4.567
200	0.454	0.758	1.428	8.233	39.743	0.163	0.515	1.079	3.733	36.712	0.256	0.514	1.075	5.981	29.230
300	0.448	1.175	5.215	37.676	121.113	0.287	1.040	3.477	28.315	99.647	0.345	0.707	4.499	31.131	217.524
400	0.808	1.755	8.150	50.572	266.936	0.290	1.510	6.634	36.709	242.583	0.497	0.992	5.888	41.564	200.256
500	1.647	2.539	11.638	67.645	239.338	0.679	1.710	9.394	34.473	155.080	0.954	1.662	8.793	47.900	297.320
GOOGL															
100	0.140	0.347	0.959	5.852	24.368	0.058	0.190	0.749	3.722	20.635	0.053	0.147	0.520	2.985	13.532
200	0.373	0.652	1.876	9.744	69.052	0.121	0.544	1.614	10.040	50.932	0.149	0.589	1.586	6.218	65.375
300	0.737	1.366	3.585	20.715	101.052	0.262	0.945	1.973	13.768	79.645	0.375	1.028	2.245	28.068	252.847
400	1.148	1.999	4.994	28.838	206.079	0.587	1.405	3.633	24.613	146.554	0.611	1.166	3.561	24.690	222.150
500	1.689	3.375	14.063	42.241	308.691	0.746	2.259	5.703	30.206	223.259	1.024	2.681	4.364	31.229	451.262
MSFT															
100	0.138	0.339	0.587	1.798	6.543	0.073	0.216	0.385	0.785	4.308	0.065	0.147	0.295	0.662	4.267
200	0.433	0.732	1.741	6.340	29.300	0.147	0.441	1.011	5.907	20.902	0.156	0.466	0.945	5.186	12.745
300	0.677	1.303	3.740	9.406	51.728	0.160	0.864	2.123	10.985	40.696	0.244	0.753	1.864	10.098	44.484
400	0.804	2.243	4.359	29.174	118.647	0.303	1.173	3.858	24.152	80.477	0.674	1.114	4.183	34.156	160.402
500	1.611	2.736	6.654	34.097	166.427	0.855	2.343	5.563	28.722	97.147	1.123	2.121	4.850	25.421	309.426
ℓ_2 norm															
AAPL															
100	0.104	0.203	0.679	1.965	4.969	0.062	0.160	0.415	1.205	3.217	0.034	0.170	0.350	0.844	3.663
200	0.250	0.629	1.598	8.360	31.688	0.150	0.374	1.487	5.628	12.848	0.184	0.360	0.839	5.201	13.667
300	0.394	1.169	3.236	8.267	79.331	0.265	0.964	1.817	7.653	35.220	0.289	0.853	1.714	5.183	22.367
400	0.588	3.600	4.145	7.281	62.433	0.404	1.295	2.764	6.175	21.839	0.429	1.020	3.666	10.928	30.042
500	1.099	3.723	15.926	29.538	52.431	0.530	2.266	3.560	8.962	57.920	0.625	1.903	2.646	8.291	48.734
AMZN															
100	0.109	0.218	0.286	0.777	1.179	0.076	0.148	0.247	0.427	1.161	0.062	0.157	0.221	0.478	0.831
200	0.258	0.424	1.218	2.130	5.701	0.139	0.438	0.646	1.383	7.166	0.148	0.382	0.846	1.586	5.873
300	0.484	0.988	2.767	16.382	19.382	0.348	1.005	2.751	8.527	24.557	0.237	0.749	1.729	8.916	10.793
400	0.400	1.832	4.465	23.897	73.663	0.507	1.360	4.759	8.792	49.129	0.340	1.614	3.215	12.222	23.187
500	0.712	2.756	5.895	26.423	41.180	0.458	2.096	4.560	17.507	36.219	0.385	2.009	3.743	8.992	40.917
GOOGL															
100	0.115	0.152	0.407	1.913	6.345	0.069	0.175	0.440	1.392	3.649	0.061	0.172	0.309	0.847	4.056
200	0.194	0.561	0.769	3.801	11.515	0.114	0.494	1.147	1.863	9.901	0.109	0.371	0.660	1.747	6.195
300	0.994	2.632	4.238	13.792	36.958	0.247	0.748	1.948	8.475	13.250	0.224	0.583	1.783	4.783	10.418
400	0.572	1.002	4.119	16.343	74.098	0.334	1.498	3.035	14.312	36.088	0.424	1.308	2.533	10.149	28.028
500	0.945	1.772	5.478	11.159	81.679	0.568	1.821	2.784	14.268	49.079	0.458	1.427	3.206	10.104	87.193
MSFT															
100	0.105	0.220	0.333	0.660	1.484	0.055	0.129	0.274	0.566	1.623	0.054	0.103	0.277	0.347	1.078
200	0.164	0.478	1.043	1.912	4.975	0.106	0.390	0.832	1.871	6.445	0.112	0.256	0.638	1.211	2.572
300	1.661	2.117	2.636	12.467	21.810	0.249	0.832	1.973	3.845	9.509	0.254	0.569	1.695	3.182	7.971
400	1.978	1.831	10.261	16.600	29.522	0.498	1.259	3.111	6.701	18.756	0.413	1.257	2.156	9.118	14.702
500	0.676	4.218	13.728	23.204	54.431	3.611	1.597	4.090	13.734	60.155	0.570	1.791	2.332	8.310	34.650

Bracketed values [] denote integrality gaps when the solver reached the 2000 s time limit.

A.6 Computational Results for Univariate Piecewise Linear Fitting with Continuity

Table 4: Comparison of runtimes (in seconds) for the Basic, Alternate, Extended Basic, and Extended Alternate formulations for univariate continuous PWL fitting. Results corresponding to ℓ_1 and ℓ_2 losses are reported sequentially. Bold entries mark the fastest formulation, and bracketed values denote integrality gaps when the 2000 s time limit is reached.

T	K=2	K=3	Basic			K=5	K=2	K=3	Alternate			K=5	K=2	Extended Basic			K=5	K=2	K=3	Extended Alternate			K=5
			K=4	K=4	K=4		K=4	K=4	K=4	K=4	K=4			K=4	K=4	K=4				K=4	K=4	K=4	
ℓ_1 objective																							
AAPL																							
100	0.200	0.669	2.237	25.772	0.141	0.739	2.939	55.465	0.221	0.761	1.697	35.525	0.126	0.719	2.232	50.734							
200	0.542	1.549	22.770	[0.423%]	0.308	2.176	37.332	919.904	0.859	2.167	23.755	713.449	0.283	1.671	38.115	1198.870							
300	0.890	3.173	444.490	[0.598%]	0.652	5.744	270.792	1978.423	1.023	4.104	73.111	729.937	0.585	5.195	201.416	[1.964%]							
400	1.027	11.442	184.113	[1.264%]	0.974	20.490	345.078	[21.189%]	1.594	7.754	125.965	[7.415%]	1.024	18.465	334.594	[13.773%]							
500	1.647	6.523	[0.046%]	[0.861%]	1.336	11.195	868.189	[25.545%]	1.940	6.322	114.502	[0.147%]	1.312	18.788	582.481	[16.235%]							
AMZN																							
100	0.241	0.470	1.955	7.205	0.161	0.828	5.210	22.339	0.323	0.754	2.255	9.731	0.156	0.695	3.200	20.963							
200	0.805	1.952	44.411	1895.353	0.503	2.261	43.847	756.499	0.691	3.440	28.377	351.404	0.477	2.300	34.339	727.409							
300	0.919	2.772	706.374	[0.590%]	0.662	2.828	107.094	1348.750	1.044	2.692	44.940	424.461	0.726	3.101	92.366	954.073							
400	2.397	4.128	55.694	1304.122	1.078	7.852	76.838	[5.078%]	1.831	4.220	29.608	499.354	1.055	6.533	65.452	[1.602%]							
500	1.453	37.587	347.259	[0.762%]	1.165	39.649	153.052	[2.094%]	3.216	19.026	201.970	1535.408	1.164	37.841	167.399	[2.774%]							
GOOGL																							
100	0.141	0.712	6.623	33.735	0.142	0.920	7.891	76.340	0.243	1.237	5.795	55.804	0.135	0.881	8.020	70.390							
200	0.711	1.420	5.146	70.631	0.550	1.951	15.772	369.903	0.930	1.536	5.064	67.524	0.536	1.275	10.120	336.650							
300	1.957	3.076	358.136	115.368	0.934	4.675	173.541	1199.054	1.358	4.153	111.457	145.774	0.860	4.534	189.503	470.250							
400	1.555	7.136	[0.056%]	[0.229%]	1.195	7.560	349.335	[2.819%]	2.085	5.819	278.491	801.831	1.114	8.771	401.726	[7.047%]							
500	2.145	17.616	514.252	[2.043%]	1.788	33.043	718.246	[12.554%]	3.619	26.056	325.506	[0.484%]	1.810	40.376	914.950	[14.934%]							
JNJ																							
100	0.196	0.961	5.802	64.889	0.171	0.972	8.491	74.058	0.235	0.894	7.191	37.588	0.127	0.779	8.207	60.709							
200	0.774	1.757	10.934	200.091	0.369	2.455	20.198	585.048	0.710	2.098	16.372	175.571	0.333	1.613	20.726	345.812							
300	1.262	6.377	196.134	947.287	0.626	11.311	104.010	1389.036	0.765	4.640	41.486	305.036	0.637	6.540	115.796	1576.151							
400	1.552	10.453	[0.728%]	[1.695%]	1.121	23.254	413.406	[9.280%]	1.392	10.991	311.155	[0.628%]	0.762	18.502	520.374	[5.971%]							
500	3.703	9.844	1078.170	[2.977%]	1.589	24.641	800.254	[22.265%]	1.492	8.513	149.358	[7.396%]	1.306	24.019	826.918	[19.694%]							
MSFT																							
100	0.161	0.618	4.604	56.349	0.157	0.726	7.986	59.991	0.243	0.703	6.164	25.692	0.174	0.488	5.430	49.287							
200	0.677	2.006	9.089	184.493	0.421	1.817	28.175	743.201	0.635	1.441	11.935	579.406	0.403	1.663	35.099	711.249							
300	0.907	3.547	549.421	1122.915	0.682	6.409	258.123	513.699	0.862	3.502	130.000	196.837	0.667	5.955	304.209	857.004							
400	1.709	7.866	318.877	[1.028%]	1.399	15.922	245.835	1609.853	1.872	6.560	[0.071%]	702.760	0.963	13.809	305.106	[7.730%]							
500	1.888	64.305	320.174	[4.659%]	1.403	54.332	449.264	[29.727%]	2.632	18.731	732.682	[7.559%]	1.433	38.591	440.320	[20.355%]							
ℓ_2 objective																							
AAPL																							
100	0.226	0.875	1.769	27.191	0.152	0.810	3.204	57.949	0.277	1.083	1.660	26.606	0.117	0.360	0.851	18.271							
200	0.640	7.140	19.220	1011.833	0.377	2.424	40.373	1131.186	0.888	4.840	28.275	382.013	0.282	1.408	13.618	349.028							
300	0.984	65.472	724.806	1460.753	0.707	5.019	160.875	[8.718%]	1.367	10.387	150.447	287.130	0.449	4.720	88.961	[9.678%]							
400	1.769	73.240	223.282	[2.901%]	1.101	16.040	457.354	[29.652%]	1.987	23.196	207.625	[0.997%]	0.841	22.871	257.998	[18.604%]							
500	2.175	110.761	[0.028%]	[0.883%]	1.302	11.015	956.308	[18.793%]	2.384	12.669	499.778	[0.014%]	1.455	7.317	352.459	[23.903%]							
AMZN																							
100	0.231	0.906	3.024	6.295	0.112	0.721	1.444	2.361	0.264	0.786	1.727	4.282	0.106	0.475	1.776	1.926							
200	0.834	14.007	176.618	[0.017%]	0.245	2.872	37.102	150.137	1.097	10.159	38.192	280.835	0.236	3.336	19.447	258.868							
300	1.015	4.895	77.100	[0.030%]	0.566	2.806	22.869	417.935	1.412	4.420	30.853	182.851	0.582	1.929	39.267	457.130							
400	2.047	10.640	182.574	[1.624%]	1.055	5.667	69.037	711.540	2.795	6.291	87.830	[0.869%]	1.212	5.797	25.638	1095.831							
500	1.798	110.761	[0.028%]	[0.883%]	1.494	29.856	709.967	[18.561%]	3.368	36.810	[0.412%]	[5.143%]	1.421	29.559	588.678	[11.623%]							
GOOGL																							
100	0.203	1.010	76.608	89.229	0.107	0.758	9.366	75.742	0.210	1.065	15.082	107.713	0.119	0.461	6.294	38.904							
200	0.634	1.824	4.901	31.388	0.313	1.927	3.582	71.380	1.093	1.267	6.159	47.484	0.302	0.591	2.728	27.544							
300	1.007	59.428	306.861	490.462	0.605	4.275	97.066	133.590	1.130	13.289	84.129	217.098	0.631	4.454	115.441	220.268							
400	1.381	240.679	169.520	[0.075%]	0.884	7.936	161.107	181.981	2.309	35.082	174.630	1194.917	0.883	8.159	279.228	282.096							
500	4.926	81.828	[0.297%]	[1.308%																			

A.7 Computational Results for Multidimensional Multiple Change-point Detection

Table 5: Comparison of runtimes (in seconds) for the Basic, Alternate, and Extended formulations for multidimensional change-point detection. Results corresponding to ℓ_1 and ℓ_2 losses are reported sequentially. Bold entries mark the fastest formulation, and bracketed values denote integrality gaps when the 2000 s time limit is reached.

T	Basic					Alternate					Extended				
	D=2	D=4	D=6	D=8	D=10	D=2	D=4	D=6	D=8	D=10	D=2	D=4	D=6	D=8	D=10
ℓ_1 norm															
$K = 2$															
100	0.224	0.396	0.358	0.452	0.635	0.159	0.222	0.356	0.403	0.493	0.129	0.198	0.342	0.320	0.414
200	0.633	0.909	1.301	1.865	2.762	0.187	0.597	0.684	1.064	1.530	0.195	0.524	0.847	0.954	1.384
300	0.826	1.563	2.062	2.790	3.177	0.457	1.088	1.309	1.821	2.724	0.619	1.094	1.875	2.416	2.698
400	1.519	1.750	3.204	6.429	6.349	0.726	1.316	2.488	4.957	3.058	0.799	1.472	2.581	3.326	4.816
500	1.852	3.412	13.668	7.873	10.906	0.873	1.959	3.249	4.814	6.916	0.921	3.013	3.342	5.069	7.052
$K = 3$															
100	0.489	0.874	1.234	1.884	2.869	0.386	0.676	1.211	1.868	1.796	0.316	0.593	0.741	1.127	1.983
200	1.375	2.228	3.365	5.319	7.251	0.996	1.780	2.219	3.605	0.740	1.627	3.114	4.035	6.310	
300	1.926	4.511	5.689	9.149	12.947	1.537	2.324	5.661	5.884	9.462	1.263	3.003	4.286	7.348	10.170
400	3.186	7.235	13.536	19.994	23.354	2.104	6.743	11.098	14.553	17.476	3.011	5.254	10.894	11.902	15.725
500	5.323	9.585	15.036	35.301	39.144	4.076	6.343	21.594	25.169	34.639	4.227	8.111	14.691	22.399	30.692
$K = 4$															
100	1.254	2.130	4.771	6.320	8.529	0.662	1.656	3.462	4.155	6.562	0.717	1.357	3.235	4.394	8.540
200	3.374	7.231	13.108	17.809	18.054	2.266	6.119	13.634	14.814	18.747	3.440	5.275	8.640	18.822	15.754
300	8.302	19.742	21.764	44.679	46.200	5.322	13.904	18.968	30.775	5.697	15.032	25.657	35.123	46.317	
400	11.894	25.138	85.169	63.508	90.823	8.840	25.097	72.275	77.125	89.082	9.359	40.103	34.737	50.717	82.045
500	33.855	53.170	184.480	92.463	139.914	12.469	58.929	117.057	136.564	111.722	15.228	65.113	117.122	103.588	139.888
$K = 5$															
100	3.449	11.554	25.494	31.254	63.585	2.278	9.504	28.996	29.890	60.469	2.557	5.495	24.563	31.745	71.990
200	9.758	30.784	46.467	69.014	125.973	7.299	32.686	49.607	72.348	176.104	6.496	25.602	71.538	61.538	137.494
300	52.498	107.522	187.144	242.354	270.022	47.058	106.067	156.311	218.424	426.947	39.029	85.226	124.624	209.227	449.540
400	41.554	201.235	308.397	611.627	804.455	36.176	177.657	401.923	522.096	991.272	60.835	141.643	512.897	819.378	568.900
500	87.467	293.485	1081.271	923.532	989.204	59.256	236.190	776.684	1286.894	1788.948	59.433	230.421	701.791	1122.924	1019.004
ℓ_2 norm															
$K = 2$															
100	0.136	0.239	0.306	0.373	0.528	0.120	0.227	0.390	0.698	0.554	0.110	0.205	0.339	0.396	0.787
200	0.428	0.949	1.464	1.221	4.862	0.291	0.597	0.883	1.612	1.666	0.285	0.698	1.291	1.407	1.576
300	1.261	1.267	12.153	3.908	11.426	0.824	3.143	4.087	2.757	3.056	0.822	1.182	2.059	2.761	5.113
400	1.626	2.415	5.112	6.181	13.252	1.319	2.455	4.804	5.015	29.653	0.786	2.694	3.798	4.895	7.182
500	2.071	9.867	6.818	13.512	21.946	1.645	3.186	4.622	12.174	8.813	0.996	3.144	4.652	8.144	7.673
$K = 3$															
100	0.335	0.667	0.780	1.187	1.494	0.250	0.537	0.959	1.477	1.659	0.286	0.397	1.026	1.247	1.584
200	1.174	2.190	5.497	5.284	6.395	0.617	1.682	3.350	5.436	5.987	0.840	2.714	3.229	3.027	5.788
300	2.776	2.664	11.554	13.145	9.156	2.165	4.785	5.580	9.050	9.927	1.538	4.480	7.615	10.623	8.988
400	3.019	7.583	10.661	19.716	16.075	2.908	7.160	9.235	13.021	9.598	3.007	5.690	9.534	16.698	34.477
500	5.953	14.455	27.333	29.442	50.015	3.314	8.381	21.195	35.868	25.963	3.326	11.265	18.305	23.059	31.459
$K = 4$															
100	0.549	1.633	2.204	4.154	5.818	0.425	1.180	1.934	2.695	5.191	0.353	0.757	2.175	3.532	3.691
200	2.996	6.908	6.966	12.918	11.604	1.621	5.837	4.384	8.523	14.848	2.027	4.608	5.386	10.307	17.108
300	4.742	22.653	20.914	30.844	55.479	3.000	11.099	20.927	31.000	38.921	5.721	10.516	18.618	27.812	39.393
400	13.025	36.098	41.978	45.713	71.282	6.247	12.023	35.362	46.989	81.521	7.898	22.749	38.945	71.777	54.106
500	12.390	48.537	89.892	64.689	180.159	13.479	23.605	68.433	72.018	93.042	10.762	26.439	63.156	103.583	95.948
$K = 5$															
100	1.528	2.880	10.057	10.454	20.752	1.116	2.755	5.155	7.983	24.197	1.129	2.714	5.472	9.723	22.687
200	5.595	7.958	24.368	20.327	56.828	3.101	6.520	18.312	19.558	53.700	4.255	5.391	18.666	15.880	62.265
300	20.575	42.364	83.044	85.714	132.573	11.401	44.040	80.363	102.743	106.218	12.123	63.869	84.319	71.539	160.278
400	35.520	80.978	175.262	229.775	299.969	26.076	79.579	166.780	265.245	342.733	19.140	102.366	236.995	380.372	281.627
500	56.201	112.584	208.046	266.936	418.571	29.325	111.372	274.412	299.463	459.186	18.347	90.802	189.875	293.481	497.909

Bracketed values [·] denote integrality gaps when the solver reached the 2000 s time limit.

A.8 Stock Indices Used in Sparse Change-Point Detection Experiments

The stock indices used in the sparse change-point detection experiments consists of a fixed, ordered list of large-cap U.S. equities primarily drawn from the S&P 100 index. The ordering of tickers is held constant across all experiments. When constructing a D -dimensional signal, the first D stocks from this list are selected. The complete list of tickers, in order, is as follows:

No.	Ticker	No.	Ticker	No.	Ticker	No.	Ticker
1	AAPL	2	MSFT	3	AMZN	4	GOOGL
5	META	6	NVDA	7	TSLA	8	BRK-B
9	JPM	10	JNJ	11	V	12	PG
13	XOM	14	MA	15	UNH	16	HD
17	BAC	18	PFE	19	KO	20	DIS
21	CSCO	22	VZ	23	ADBE	24	NFLX
25	CRM	26	INTC	27	CMCSA	28	ABT
29	T	30	AVGO	31	TMO	32	NKE
33	MRK	34	WMT	35	CVX	36	MCD
37	COST	38	ORCL	39	QCOM	40	WFC
41	ACN	42	DHR	43	BMY	44	MDT
45	TXN	46	PM	47	HON	48	IBM
49	UNP	50	SBUX	51	AMGN	52	AMD
53	CAT	54	LOW	55	UPS	56	GS
57	MS	58	LLY	59	BLK	60	AMAT
61	GILD	62	PEP	63	SPGI	64	GE
65	MMM	66	BA	67	LMT	68	ADP
69	C	70	CI	71	DE	72	ISRG
73	MO	74	ZTS	75	SCHW	76	CVS
77	BK	78	USB	79	TGT	80	CB
81	INTU	82	NOW	83	MU	84	ICE
85	PLD	86	SO	87	NEE	88	ADI
89	EQIX	90	BDX	91	CL	92	FDX
93	GM	94	F	95	KMB	96	MDLZ
97	ETN	98	EOG	99	APD	100	HPQ

A.9 Computational Results for Sparse Change-point Detection

Table 6: Comparison of runtimes (in seconds) for Basic, Alternate, and Extended formulations for sparse change-point detection. Results corresponding to ℓ_1 and ℓ_2 losses are reported sequentially. Bold entries indicate the faster formulation; bracketed values denote integrality gaps when the solver reached the 2000 s time limit.

D	Basic			Alternate			Extended		
	10%	20%	30%	10%	20%	30%	10%	20%	30%
(A) ℓ_1 norm									
10	2.648	4.188	4.905	2.639	4.730	4.002	2.418	3.572	3.285
20	13.528	40.138	43.958	10.225	24.464	37.237	13.437	24.550	45.450
30	117.389	446.640	547.955	128.430	375.217	730.984	111.005	439.330	754.828
40	1293.035	[5.962%]	[4.587%]	1534.758	[6.437%]	[4.219%]	1623.543	[5.553%]	[3.837%]
(B) ℓ_2 norm									
10	3.616	4.150	4.606	2.706	3.312	3.371	3.761	4.080	4.467
20	11.758	16.097	21.704	11.435	23.409	23.141	7.769	20.036	28.151
30	65.140	86.583	133.992	94.185	165.772	144.826	82.372	150.648	170.834
40	527.653	1237.239	933.616	703.069	[5.724%]	707.586	682.605	1306.666	897.288

Bracketed values [·] denote integrality gaps when the solver reached the 2000 s time limit.